

# Structural evolution of a Mesozoic backarc fold-and-thrust belt in the U.S. Cordillera: New evidence from northern Nevada

Sandra J. Wyld<sup>†</sup>

Department of Geology, University of Georgia, Athens, Georgia 30602, USA

## ABSTRACT

Stratigraphic and structural analysis in Blue Mountain and nearby areas of northern Nevada yields new insight into the evolution of the Luning-Fencemaker fold-and-thrust belt, a Mesozoic orogenic belt that formed during tectonic closure of a Triassic backarc basin. Three stratigraphic units are defined in Blue Mountain and correlated with Upper Triassic (Norian) units in nearby areas. These units have a combined structural thickness of >6 km and consist mostly of shale (now slate and phyllite); quartzose sandstone is much less common, and carbonate is rare. Two phases of deformation affected these strata. D<sub>1</sub> deformation is pervasive and was associated with tight to isoclinal folding at various scales, widespread cleavage development under low-grade metamorphic conditions, and reverse faulting. This deformation accommodated a minimum of 55%–75% northwest-southeast shortening, with southeast-directed tectonic transport. D<sub>2</sub> deformation is only locally developed and is manifested by relatively open folds, crenulations, and a spaced cleavage. This phase of deformation accommodated a minor amount of northeast-southwest shortening and was not accompanied by metamorphism. Structures and deformation phases in Blue Mountain can be correlated with those found in nearby areas. The D<sub>1</sub> phase of deformation is pronounced across the entire northern part of the Luning-Fencemaker fold-and-thrust belt and resulted in structural closure of the backarc basin via development of a ductile fold-and-thrust belt in the Jurassic. D<sub>2</sub> is unrelated to development of the fold-and-thrust belt as a structural province and occurred much later, in the middle to Late Cretaceous. The structural evolution of this backarc fold-

and-thrust belt appears to be quite simple and did not evidently involve widespread polyphase deformation. Data from Blue Mountain and nearby areas suggest that it is now possible, for the first time, to map out megascopic structures (folds and faults) within the interior of the province.

**Keywords:** backarc basins, Blue Mountain, fold-and-thrust belts, Luning-Fencemaker, Mesozoic, Nevada.

## INTRODUCTION

The Luning-Fencemaker fold-and-thrust belt of central Nevada (Fig. 1) is an important structural province in the U.S. Cordillera for several reasons: It accommodated substantial Mesozoic shortening over a strike length of ~400 km (Fig. 1; Oldow, 1984); its development led to structural closure of a deep-marine backarc basin (basinal terrane in Fig. 1) that had dominated the paleogeography of western Nevada during the Late Triassic (Speed, 1978a; Smith et al., 1993; Wyld, 2000); it constitutes a crucial intermediate structural province between the arc terranes to the west, where deformation is largely Jurassic and verges westward, and the continent to the east, where deformation is largely Cretaceous and verges eastward (Burchfiel et al., 1992; Smith et al., 1993); and structures within it may reflect decoupling between the arc and the backarc along a bounding strike-slip fault as a result of oblique plate convergence during deformation (Oldow, 1984). The Luning-Fencemaker fold-and-thrust belt is also important from a global geology perspective because it forms an exceptionally clear-cut example of a contractional belt developed during structural closure of a backarc marine basin. An analysis of the structural evolution of this belt can therefore provide insight into the pro-

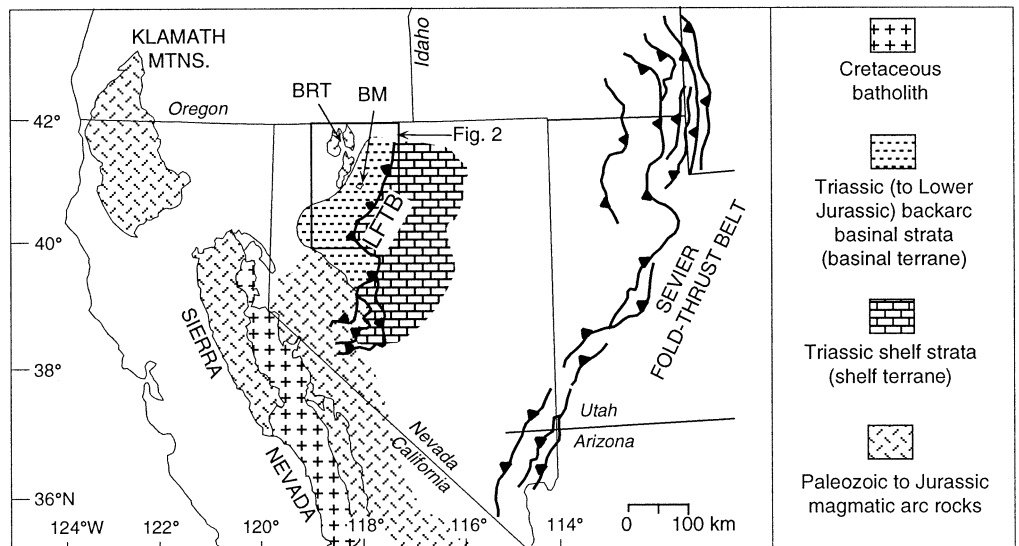
cesses by which backarc basins collapse during contractional tectonism.

Most detailed structural studies within the Luning-Fencemaker fold-and-thrust belt have been undertaken either in the south, where the backarc basin narrowed and early Mesozoic arc rocks are thrust over coeval shelf strata, or along its northeastern margin where lower Mesozoic basinal strata are thrust over coeval shelf rocks along the frontal Fencemaker thrust (Figs. 1 and 2; Speed and Jones, 1969; Speed, 1974, 1978a; Oldow, 1978; Oldow, 1984; Elison and Speed, 1989; Oldow et al., 1990). In contrast, very little is known of structural relationships in the internal part of the basinal terrane, even though this constitutes most of the Luning-Fencemaker fold-and-thrust belt (Figs. 1 and 2). One major reason for this lack of information is that the stratigraphy of basinal-terrane strata has only been established in a few areas, mostly near the Fencemaker thrust. Elsewhere, basinal-terrane rocks have been mapped only in reconnaissance and are generally lumped as one undivided unit (Willden, 1964; Johnson, 1977). This lack of any stratigraphic framework in the northern Luning-Fencemaker fold-and-thrust belt has made it impossible in many areas to discern megascopic structural features, such as map-scale folds or faults.

In this paper, I describe results of a detailed mapping, stratigraphic, and structural analysis of Blue Mountain, located in the central part of the northern Luning-Fencemaker fold-and-thrust belt (Fig. 2), and I integrate relationships from this area with those found in nearby parts of the belt in order to generate a more comprehensive model of deformation in the region. Results presented in this paper are part of a larger study involving several areas across the northern part of the fold-and-thrust belt, as discussed in Wyld (1998), Rogers (1999), Wyld et al. (1999, 2001), Folsom (2000), Wyld (2000), and Wyld and Wright (2000).

<sup>†</sup>E-mail: swyld@gly.uga.edu.

**Figure 1.** Map of the western U.S. Cordillera, showing distribution of lower Mesozoic rocks, Cretaceous batholith belt, and locations of major Mesozoic fold-and-thrust belts. The Luning-Fencemaker fold-and-thrust belt (LFTB) encompasses the entire basal terrane; only frontal thrusts are shown (Oldow, 1984). BM—Blue Mountain, BRT—Black Rock terrane.



### GEOLOGIC FRAMEWORK AND PREVIOUS WORK

The Mesozoic U.S. Cordillera can be divided into three broad geologic provinces (Fig. 1; e.g., Speed, 1978a; Burchfiel et al., 1992). To the west lie magmatic arc and related convergent-margin rocks that were either constructed on the continental margin or developed offshore of the margin. To the east, the arc was flanked in the early Mesozoic by a backarc basin (basinal terrane in Fig. 1) that developed during a period of regional extensional tectonism in the Triassic (Wyld, 2000). This basin apparently ceased to exist as a site of deep-marine deposition in the Jurassic, because no marine strata younger than Early Jurassic are known in the province (Speed, 1978a). Farther east, a shallow-marine shelf existed in the Triassic (shelf terrane of Fig. 1), but otherwise the area east of the backarc basin was continental during the Mesozoic. As shown in Figure 1, the Luning-Fencemaker fold-and-thrust belt is largely confined to the lower Mesozoic backarc basinal terrane, except in the south where the backarc basin narrowed and deformation also affected the Mesozoic arc and continental shelf. In this paper, I will only be concerned with the northern part of the fold-and-thrust belt, where deformation was restricted to the basinal terrane (Fig. 2).

The basinal terrane, originally defined by Speed (1978a), is an assemblage of dominantly deep-marine clastic strata consisting primarily of metamorphosed mudstone, with much less abundant quartz sandstone and rare carbonate (Compton, 1960; Speed, 1978a, 1978b; Lupe and Silberling, 1985; Thole and Prihar, 1998; Wyld, 2000). Biostratigraphic

data indicate that rocks of the basinal terrane are mostly of Norian (late Late Triassic) age, although locally some basinal strata of Carnian (early Late Triassic) and Early Jurassic age are known. Detailed stratigraphic studies in the northern basinal terrane were initially confined to the Santa Rosa Range and Bloody Run Hills (Compton, 1960), the west Humboldt Range (Speed, 1974), and areas adjacent to the Fencemaker thrust (Elison and Speed, 1989; Oldow et al., 1990). More recently, stratigraphic analysis of basinal-terrane rocks has been expanded to the west in the Eugene Mountains (Thole and Prihar, 1998) and Jungo area (Wyld, 2000), and the older stratigraphic information of Compton has been reexamined by Rogers (1999) and Wyld et al. (2001) in the southern Santa Rosa Range and by V. Ciararella and S.J. Wyld (work in progress) in the Bloody Run Hills. These studies consistently indicate that deposition in the basinal terrane was dominated by an influx of muddy sediments with episodic additional influxes of quartz-rich sands and minor calcareous sediments.

To the west, the northern Luning-Fencemaker fold-and-thrust belt is bounded by Paleozoic and Mesozoic magmatic arc rocks of the Black Rock terrane (Fig. 2). Although contact relationships between the two terranes are obscured by extensive Cenozoic cover, structural analyses in the Jackson Mountains and Jungo area (Fig. 2) indicate that the two terranes were likely juxtaposed along a west-dipping reverse fault in the Jurassic, during initial development of the Luning-Fencemaker fold-and-thrust belt (Quinn, 1996; Folsom, 2000; Wyld, 2000; Wyld and Wright, 2000). To the east, basinal-terrane

strata are faulted over coeval shelf rocks along the Fencemaker thrust (Fig. 2), which forms the eastern margin and frontal thrust of the northern part of the fold-and-thrust belt (Speed, 1978a; Oldow, 1984; Elison and Speed, 1989; Oldow et al., 1990). The shelf rocks, of Middle to Late Triassic age, include abundant carbonate as well as deltaic clastic sedimentary rocks (mostly mudstone and sandstone). Following the terminology originally proposed by Speed (1978a), this province is referred to as the shelf terrane. Upper Triassic clastic strata in the basinal terrane represent the deep-marine facies equivalent of coeval clastic strata of the shelf terrane, and both were derived from continental sources to the east (Lupe and Silberling, 1985; Gehrels and Dickinson, 1995; Manuszak et al., 2000).

The structural characteristics of the Luning-Fencemaker fold-and-thrust belt in the northern basinal terrane were originally defined by Oldow (1984). More recently, detailed structural studies have been completed in the southern Humboldt Range (Oldow et al., 1990), northern East Range (Elison and Speed, 1989), southern Santa Rosa Range (Rogers, 1999; Wyld et al., 2001), and the Jungo area (summaries of structural data reported in Wyld, 2000, and Wyld et al., 2002), and the broad structural framework of the Eugene Mountains has been examined (Thole and Prihar, 1998) (see Fig. 2). These studies collectively indicate that deformation in the northern Luning-Fencemaker fold-and-thrust belt involved development of a slaty to phylitic cleavage in metapelitic rocks, folding at various scales, and reverse faulting. A poly-phase sequence of structures is generally present, although the number of different defor-

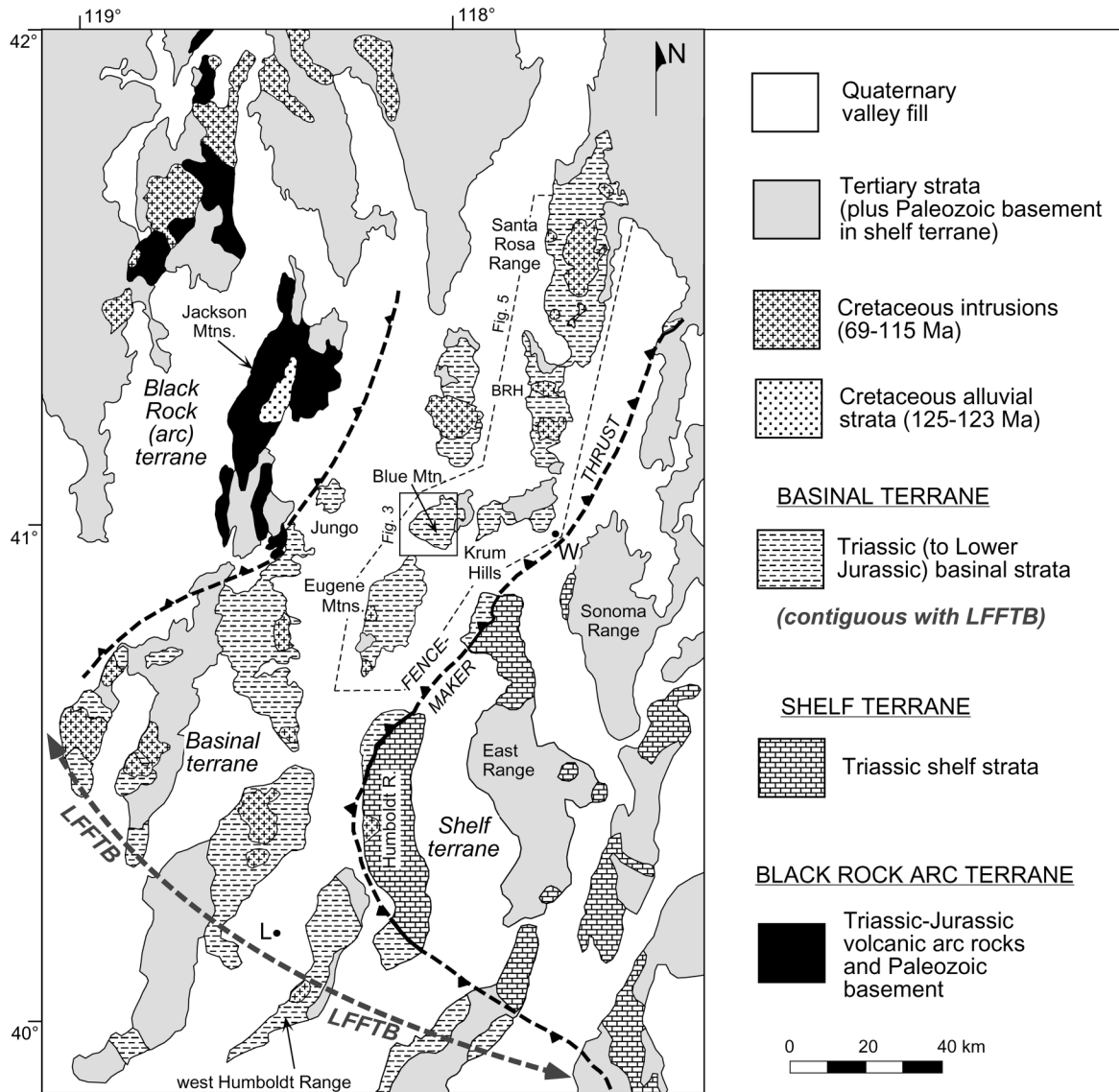


Figure 2. Location map showing mountain ranges in north-central Nevada (see Fig. 1 for location) and distribution of lower Mesozoic arc, basinal, and shelf terranes. Modified from Willden (1964), Oldow (1984), Elison and Speed (1989), Wyld (1996, 2000), and Quinn et al. (1997). BRH—Bloody Run Hills; L and W—towns of Lovelock and Winnemucca, respectively.

mational phases varies from area to area and the significance of polyphase deformation to development of the fold-and-thrust belt is not entirely clear (cf. Oldow, 1984; Elison and Speed, 1989; Wyld et al., 2001). Most shortening in the northern part of the fold-and-thrust belt was in a northwest-southeast direction on the basis of the prominent northeast-trending structural grain of deformed rocks throughout the region, and occurred prior to intrusion of Late Cretaceous granitic plutons, stocks, and dikes (Fig. 2).

Blue Mountain (Fig. 2) lies in a central location in the northern Luning-Fencemaker fold-and-thrust belt, relative to other areas in

which the stratigraphy and structural evolution have been studied in detail. It is thus an ideal site for new detailed studies, as well as a crucial one for evaluating regional patterns of deformation across and along the northern part of the fold-and-thrust belt. The geology of Blue Mountain was first described by Willden (1964) in a reconnaissance study of Humboldt County. He concluded that there were two different units in the mountain: (1) a western unit consisting of slates and phyllites of uncertain correlation with other units of the basinal terrane and (2) an eastern unit that he called the Raspberry Formation on the basis of its lithologic similarity to a Norian unit of the same

name in the shelf terrane (Nichols and Silberling, 1977). The western unit was shown by Willden (1964) to be thrust over the Raspberry Formation along a north-trending fault. The stratigraphic units, and their conjoining thrust fault, were also shown to be intruded by a dioritic stock of inferred Jurassic age.

Detailed mapping and analysis of Blue Mountain for the present study (Fig. 3) leads to the conclusion that a number of Willden's (1964) interpretations about the geology of this area are in error. First, my mapping indicates that three different stratigraphic units can be discerned in Blue Mountain, none of which corresponds directly to the units

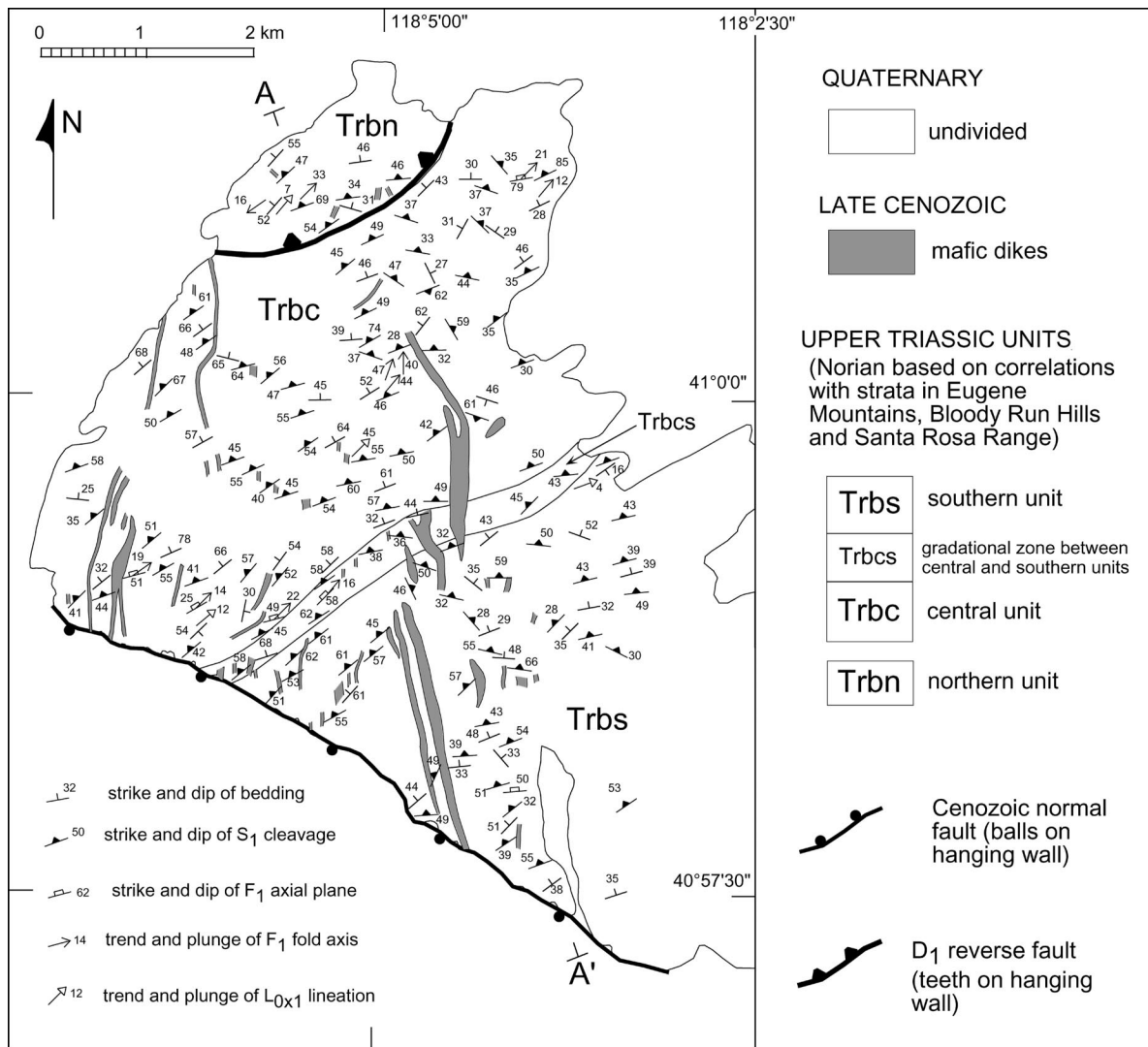


Figure 3. Geologic map of Blue Mountain. See Figure 2 for location.

mapped by Willden (1964). Second, no evidence, either structural or stratigraphic, could be found for the north-trending thrust fault shown by Willden (1964). Instead, it is clear that stratigraphic units in the mountain all trend northeast (Fig. 3) directly across the trace of Willden's inferred thrust. Third, the Jurassic(?) stock mapped by Willden (1964) does not exist. Instead, the plutonic rocks map out as a north-trending dike swarm, the largest dike of which is in the area where Willden (1964) mapped his stock. Attempts to extract zircon from rocks of this dike swarm were unsuccessful, but  $^{40}\text{Ar}/^{39}\text{Ar}$  whole-rock phyllite analyses from Blue Mountain indicate significant Ar loss in the late Cenozoic and strongly support a conclusion that elevated temperatures associated with intrusion of the dikes occurred at ca. 10 Ma (Wyld et al., 1999).

### TRIASSIC STRATIGRAPHY OF BLUE MOUNTAIN

Three stratigraphic units can be discerned in Blue Mountain (Fig. 3). These are referred to by their geographic location as the northern unit (Trbn), the central unit (Trbc), and the southern unit (Trbs). Each of these units contains abundant ( $\geq 70\%$ ) gray to black slate and phyllite, with less common quartz-rich metasandstone and metasiltstone. Despite these similarities, clear distinctions can be made between units on the basis of (1) abundance and characteristic features of metasandstone interbeds, and (2) the presence or absence of interbedded carbonate. The main features of each unit are listed in Table 1 and discussed briefly here. All units appear to have been deposited in a deep-marine environment on the

basis of the great thicknesses of metapelitic rocks and the presence of local limestone, but no attempt was made in this study to define the depositional environment of the different units in detail.

The northern unit has a structural thickness of at least 500 m and is characterized by thick to very thick bedded (1–5 m) quartzites that are more common (15%–20%) than in the other units. Northern unit quartzites are also distinctive in having the following combination of features: a composition including  $\sim 90\%$  quartz and  $\sim 5\%$  feldspar, a lack of any internal stratification features except local planar laminations, a locally developed spaced cleavage, and a scarcity or lack of any crosscutting quartz veins. Note that the presence or absence of cleavage or quartz veins in the metasandstones of Blue Mountain reflects the in-

TABLE 1. DISTINCTIVE CHARACTERISTICS OF TRIASSIC UNITS IN NORTHERN LUNING-FENCEMAKER FOLD-AND-THRUST BELT

Santa Rosa Range and Bloody Run Hills	Blue Mountain	Eugene Mountain
<u>Mullinix Formation (&gt;1500 m)</u> 65% slate, 30%–35% siltstone, 2% quartzite, rare limestone. Quartzite thin bedded. Quartzite composition: 95% Q, 2% F, 3% O	<u>Southern unit (&gt;3400 m)</u> 70%–75% slate, 10% siltstone, 15% sandstone, 3%–4% limestone and marl. Metasandstone mostly thin to medium bedded (3–50 cm, locally 1 m); with common plane laminations, cross-beds, good cleavage, no quartz veins. Metasandstone composition: 35%–65% Q, 20%–30% F, 10%–30% O	<u>Raspberry Formation (Trr; 2130 m)</u> Early late Norian pelecypods. 70%–75% slate, 2% sandstone (limy), 25% limestone and mar. Sandstones have common ripple marks, crossbeds, cast marks. Sandstone composition: feldspathic.
<u>Andorno Formation (2100–2400 m)</u> Early late Norian ammonites and pelecypods; 70%–75% slate, 10%–15% siltstone, 15% metasandstone, rare limestone and dolomite. Metasandstone mostly thin to medium bedded (2–40 cm, rarely 2 m); with common plane laminations, ripple marks, cross-beds, trace fossils, cast marks, good cleavage, no quartz veins. Metasandstone composition: 70%–75% Q, 10%–15% F, 10%–15% O	<u>Gradational zone (~400 m)</u> Gradational zone between southern and central units. 75%–80% slate and phyllite (locally limy), 10% siltstone (locally limy), 10% quartzite, 3%–4% limestone. Quartzite thin to thick bedded (1 cm–1.5 m); with massive bedding, no cleavage, some quartz veins.	<u>Triassic siliciclastic unit 2 (Trs2; 600 m)</u> Early late Norian pelecypods. 88% slate and silty slate, 8% sandstone (limy), 4% limestone. Sandstones have common ripple marks, crossbeds, plane laminations, cast marks. Sandstone composition: feldspathic.
<u>Singas Formation (1200–2100 m)</u> Norian pelecypods. 80%–85% slate, 10% siltstone, 5%–10% quartzite, rare limestone. Quartzite thin to thick-bedded (2 cm–3 m, locally 10 m); with massive bedding, no cleavage, common quartz veins. Quartzite composition: 92% Q, 5% F, 3% O	<u>Central unit (~2800 m)</u> 85% slate and phyllite (locally silty), 10% siltstone, 5% quartzite, rare limestone. Quartzite thin to thick bedded (3 cm–1 m, locally 9 m); with massive bedding or plane laminations, no cleavage, common quartz veins. Quartzite composition: 95% Q, 1%–3% F, 2%–3% O	<u>Triassic carbonate clastic unit (Trc; 15–450 m)</u> Early late Norian pelecypods. Mostly limestone, less common dolomite.
<u>O'Neill Formation (0–600 m)</u> Pinches out to northwest. 65% slate and phyllite, 15%–20% siltstone, 15%–20% quartzite. Quartzite mostly thick to very thick bedded (2–6 m, varies from 30 cm to 15 m); with massive bedding or plane laminations, good cleavage, rare quartz veins. Quartzite composition: 85% Q, 3%–5% F, 10% O	<u>Northern unit (&gt;500 m)</u> 70%–75% phyllite, 10% siltstone, 15%–20% quartzite. Quartzite mostly thick to very thick bedded (1–5 m; varies from 3 cm to 8m); with massive bedding, variable cleavage, rare quartz veins. Quartzite composition: 90%Q, 3%–5% F, 5% O	<u>Triassic siliciclastic unit 1 (Trs1; 2440 m)</u> Early late Norian pelecypods. 66% slate and phyllite, 20% siltstone, 12% quartzite, 2% limestone. Quartzite thin to very thick bedded (30 cm to 15 m), with mostly massive bedding. Quartzite composition: very pure, typically with only 1%–2% F.
<u>Winnemucca Formation (180–450 m)</u> Middle Norian ammonites. 55% slate (variably limy), 25%–30% siltstone (variably limy), 1%–2% quartzite, 10%–15% limestone. Quartzite thin-bedded.		<u>Pelitic metasedimentary unit (unit Trms; &gt;900 m)</u> Late early and middle Norian ammonites. 70% slate and phyllite, 18% siltstone, 10%–15% quartzite, 2% limestone. Quartzite thin to very thick bedded (several centimeters to 15 m).
<u>Grass Valley Formation (&gt;300 m)</u> 90%–95% slate and phyllite, 5%–10% quartzite. Quartzite thin to thick bedded (2 cm–3 m, up to 20 m); with massive bedding, variable cleavage, common quartz veins. Quartzite composition: 95% Q, 2%–4% F, 1%–2% O		

*Note:* Data sources for Santa Rosa Range and Bloody Run Hills (Compton, 1960; Rogers, 1999; Wyld et al., 2001), Blue Mountain (this study), Eugene Mountains (Thole and Prihar, 1998). Percentages of different rock types are approximate. Abbreviations for metasandstone compositions: Q—quartz; F—feldspar (mostly or entirely plagioclase); O—other grains, which include some combination of muscovite, chlorite, calcite, opaque material, and/or actinolite. Detailed data on metasandstone compositions are not available from the Eugene Mountains.

fluence of composition on sandstone rheology during deformation (see section on  $D_1$  deformation) and can be effectively used as a diagnostic tool to distinguish units in the northern basinal terrane (cf. Compton, 1960; Rogers, 1999; Wyld, 2000).

The central unit has a structural thickness of ~2800 m and is characterized by a predominance of slate and phyllite (~95% of unit), thinly interlayered in places with metasiltstone, and scarce quartzite interbeds. Quartzites in this unit are distinctive in having the following combination of features: a very clean and quartz-rich composition including ~95% quartz and 1%–3% feldspar; highly

variable bed thickness, from a few centimeters to 9 m; a lack of any internal stratification features except local planar laminations; and an abundance of crosscutting quartz veins in most beds and a lack of any tectonic cleavage. There are also some rare limestone interbeds in this unit. The contact between the northern and central units appears to be a fault, on the basis of structural relationships described in a later section.

The southern unit has a structural thickness of at least 3400 m and is characterized by a greater abundance of interbeds of nonpelitic rocks than the other units, including ~15% metasandstone, 10% metasiltstone, and 3%–

4% limestone and calcareous slate. Metasandstones in this unit are also distinctive in the following combination of features: They are mostly thin to medium bedded (3–50 cm); they contain ~10%–30% matrix (now recrystallized to quartz + actinolite + calcite + chlorite); their clast population includes 20%–30% feldspar with only 35%–65% quartz; they contain abundant internal stratification features, including cross-beds and planar laminations; and they typically have a well-developed spaced cleavage but no crosscutting quartz veins. Between the central and southern units, there is a gradational zone ~400 m wide in which the rock assemblage shares

some characteristics of both units (unit Trbc; Fig. 3; Table 1), which led me to interpret the central and southern units are in conformable and gradational contact.

Bedding in the units of Blue Mountain dips predominantly to the northwest (Fig. 3), suggesting that units may young in that direction. This conclusion warrants careful examination, however, because Triassic units in the Eugene Mountains, just to the south of Blue Mountain (Fig. 2), also dip to the northwest but are entirely overturned (Thole and Prihar, 1998). Available data from within Blue Mountain does not resolve this problem. No datable fossils were found in any of the units. There is also a notable lack of any internal stratification features in the metasedimentary rocks that could provide a clear indication of the original "up" direction, and, even if these features were more abundant, they would have limited use because of the common presence of tight to isoclinal folds of bedding in the rocks (see section on  $D_1$  deformation). Finally, the angle between cleavage and bedding in Blue Mountain cannot be used to discern whether units are upright or overturned because cleavage is, on average, subparallel in orientation to bedding within the units (Fig. 3). It is possible, however, to correlate the three units in Blue Mountain with dated units in nearby parts of the basinal terrane, as explained in the following section. This analysis indicates that the units in Blue Mountain are overturned.

**REGIONAL CORRELATION OF BLUE MOUNTAIN UNITS AND STRUCTURAL IMPLICATIONS**

The most logical areas to consider in terms of correlation for Blue Mountain units are the Santa Rosa Range and Bloody Run Hills to the northeast and the Eugene Mountains to the southwest (Figs. 2 and 4), because (1) these areas are very close to Blue Mountain and along strike from it (basinal-terrane units in all areas strike northeast and dip northwest), and (2) their stratigraphy has been established at a level of detail that facilitates comparisons (Compton, 1960; Thole and Prihar, 1998; Rogers, 1999; Wyld et al., 2001). Key characteristics of the basinal-terrane units in these areas are listed in Table 1, where they can be compared with the characteristics of the three units in Blue Mountain. Simplified stratigraphic columns of the Triassic units of the Santa Rosa Range, Bloody Run Hills, and Eugene Mountains are shown in Figure 5, along with the three units in Blue Mountain organized vertically to emphasize reasonable cor-

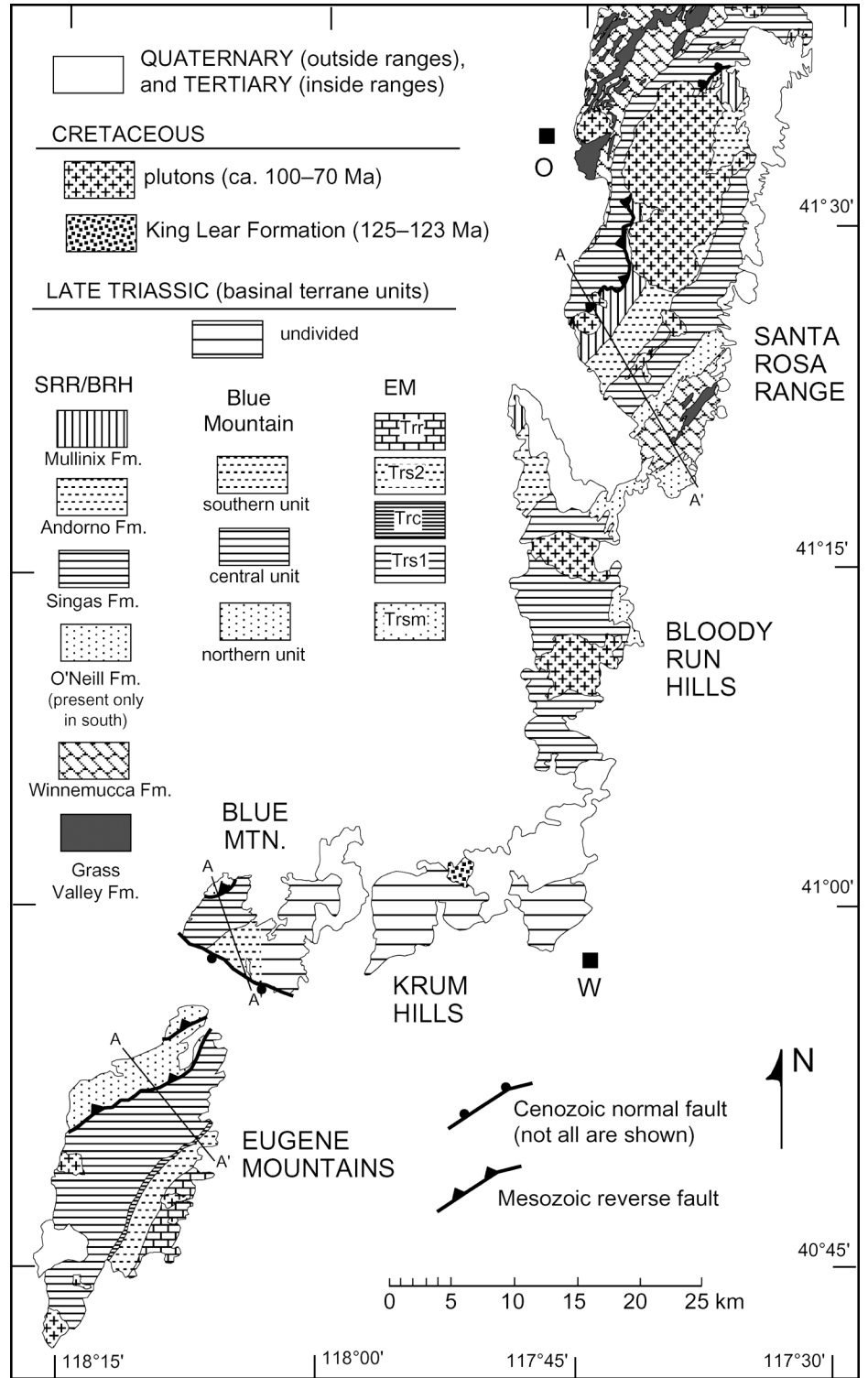


**Figure 4. Geologic map of the Santa Rosa Range and Bloody Run Hills (Compton, 1960; Rogers, 1999; Wyld et al., 2001), Krum Hills (Willden, 1964), Blue Mountain (this study), and Eugene Mountains (Thole and Prihar, 1998). See Figure 2 for location. In stratigraphic legend of Triassic units, EM is Eugene Mountains, and SRR/BRH is Santa Rosa Range and Bloody Run Hills. O and W are towns of Orovada and Winnemucca, respectively.**

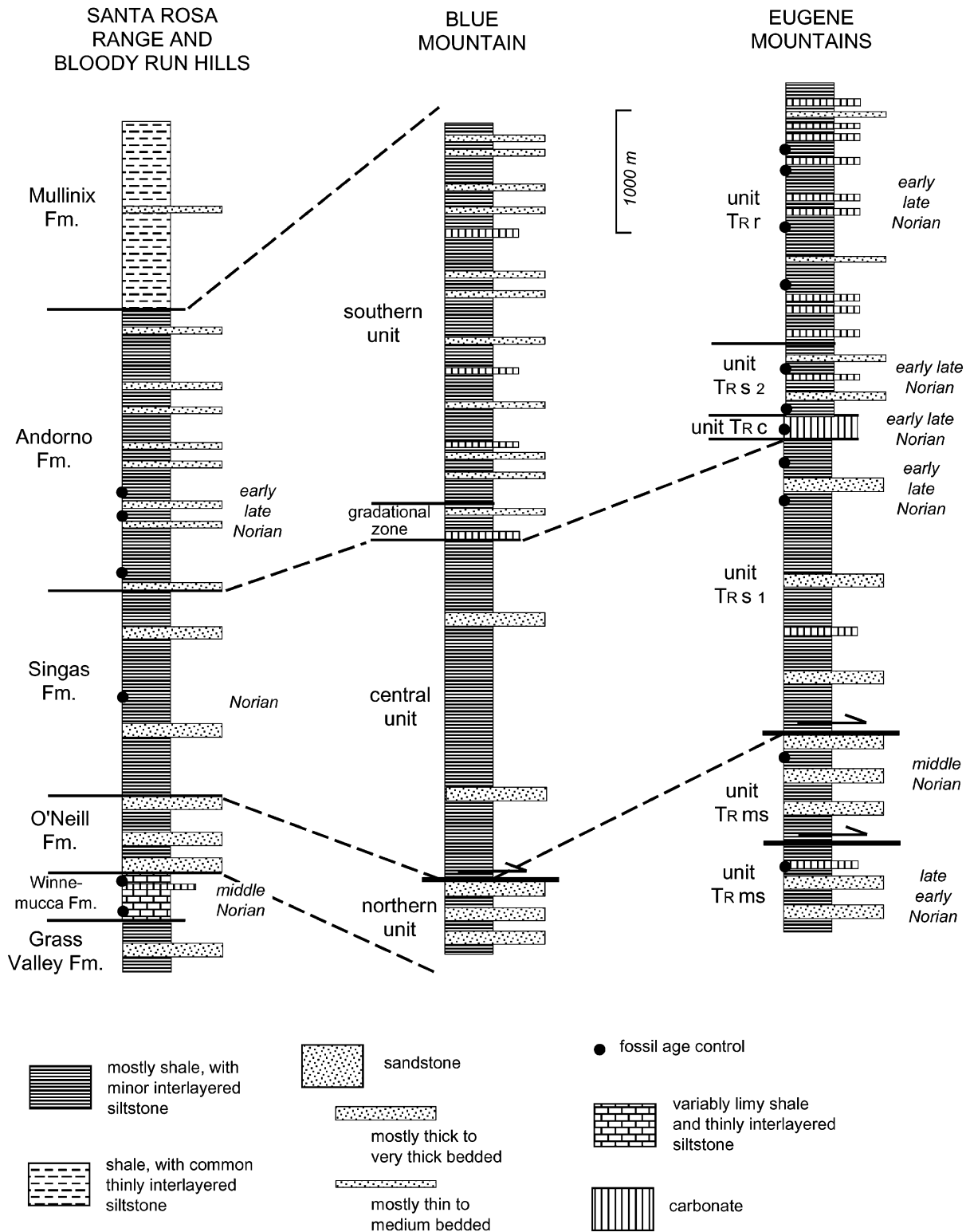
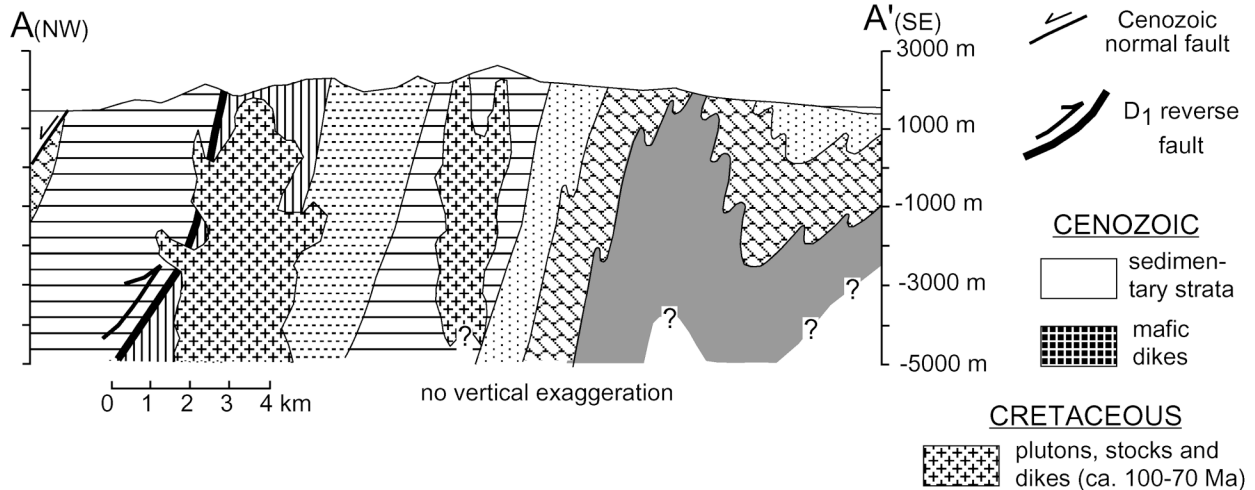
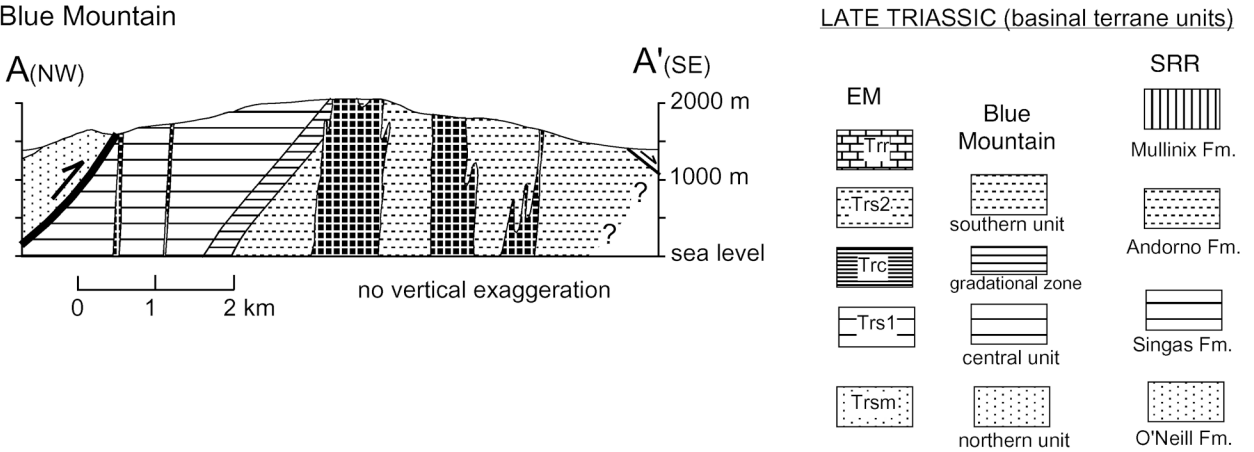


Figure 5. Schematic stratigraphic columns for Mesozoic units of the Santa Rosa Range and Bloody Run Hills (Compton, 1960; Rogers, 1999), Blue Mountain (this study), and Eugene Mountains (Thole and Prihar, 1998). Columns are designed to show structural thickness of units, relative proportion of different rock types in each unit, relative thickness of bedding in sandstones of each unit, and approximate level of age-diagnostic fossils (see Table 1 for additional information), but are not intended to represent measured sections. Inferred correlations between units in the different areas shown by dashed lines. Stratigraphic stacking order shown for Blue Mountain units is based on inferred correlations with units in the other areas. See text for discussion.

A. southern Santa Rosa Range



B. Blue Mountain



C. Eugene Mountains

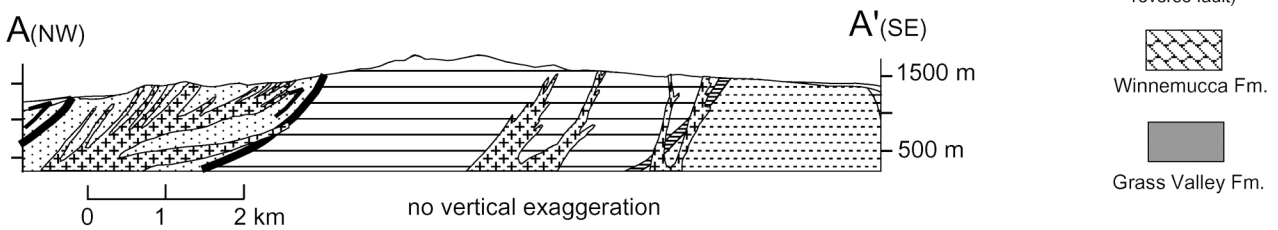


Figure 6. Structure sections through (A) the southern Santa Rosa Range (Rogers, 1999; Wyld et al., 2001), (B) Blue Mountain (this study), and (C) the Eugene Mountains (Thole and Prihar, 1998). See Figures 3 and 4 for locations of structure sections. Note that the scale of the Blue Mountain and Eugene Mountain sections is twice that of the scale of the southern Santa Rosa Range section.

relations with the other areas. Structure sections through the southern Santa Rosa Range, the Blue Mountain, and the Eugene Mountains are shown in Figure 6, in order to compare the megascopic structural and stratigraphic architecture of the various areas.

As in Blue Mountain, basinal-terrane units in the other areas consist mostly of slate and phyllite (generally >65%), with variably less common quartz-rich metasediments, metasilstone, and/or carbonate. The units are distin-

guished in a way similar to those in Blue Mountain—i.e., by the abundance and characteristics of metasandstone interbeds and by the abundance of carbonate. Ages of units in the Santa Rosa Range, Bloody Run Hills, and Eugene Mountains are based on fossil pelecypods and ammonites (Table 1; Compton, 1960; Lupe and Silberling, 1985; Thole and Prihar, 1998). All of the dated units are Norian (latest Triassic); the oldest units contain fossils of late early and middle Norian age, and the

youngest units contain fossils whose age is Norian or early late Norian (Fig. 5).

Correlations between Blue Mountain and the Santa Rosa Range and Bloody Run Hills are most obvious because of my extensive work mapping in all of these areas. Three units share clear similarity between the areas. The northern unit in Blue Mountain is very similar to the O'Neill Formation (Table 1, Fig. 5): metasediments in both units are quartzites with ≤5% feldspar; abundance of quartzite in-

terbeds in both units is similar (15%–20%); and quartzites in both units are typically thick to very thick bedded, massive or planar laminated, lacking in crosscutting quartz veins, and deformed to some extent by a spaced cleavage. The central unit in Blue Mountain is very similar to the Singas Formation (Fig. 5, Table 1): both are dominated (90%–95%) by slate and phyllite, with some thinly interlayered metasilstone; both contain rare limestone interbeds; metasandstones in both are extremely rich in quartz (~95%), are typically cut by many quartz veins, and do not display any tectonic cleavage; and the quartzites in both units occur in beds that vary widely in thickness (from 2 cm to 10 m) and are either massive or planar laminated. Finally, the southern unit in Blue Mountain is very similar to the Andorno Formation (Fig. 5, Table 1): both contain 15% metasandstone and 10%–15% metasilstone, with some carbonate interbeds; metasandstones in both units contain significant feldspar as well as quartz and show a well-developed spaced cleavage but no quartz veins; and metasandstones in both are generally thin to medium bedded with relatively common current markings, including cross-beds and planar lamination. The only significant differences between the Andorno Formation and the southern unit are that the latter contains more carbonate interbeds and its sandstones contain a greater percentage of feldspar. On the basis of this analysis, I conclude that the northern, central, and southern units of Blue Mountain are likely correlative, respectively, with the O'Neill, Singas, and Andorno Formations of the Santa Rosa Range and Bloody Run Hills.

Probable correlations can also be made between the three Blue Mountain units and those defined just to the south in the Eugene Mountains (Fig. 5; Thole and Prihar, 1998), although there is less detailed information from the latter area to use as a basis for correlation. The northern unit in Blue Mountain appears very similar to unit Trms in the Eugene Mountains (Fig. 5, Table 1), in that both contain ~15% quartzites that are commonly thick to very thick bedded. The only obvious difference between the units is that Trms contains ~2% limestone, whereas no limestone is observed in the northern unit. The central unit in Blue Mountain appears quite similar to unit Trs1 in the Eugene Mountains. Like the former, unit Trs1 is characterized by a predominance of slate and phyllite, with thinly interlaminated siltstone, rare limestone, and only minor quartzite interbeds (~5% in most areas); the quartzites are very pure (usually with only 1%–2% feldspar); and the quartzites oc-

cur as thin- to medium-bedded lenses as well as thick to very thick channel deposits. The principal differences between the two units is that Trs1 contains somewhat more limestone (2%) than the central unit (<1%).

Potential correlations between the southern unit in Blue Mountain and units in the Eugene Mountains are somewhat less clear. The southern Blue Mountain unit is unlike either units Trs1 or Trms in the Eugene Mountains, and it is also unlike the carbonate-dominated unit Trc. It is, however, similar in certain key respects to units Trs2 and/or Trr (Fig. 5, Table 1): all contain calcareous interbeds, all contain feldspar-rich metasandstones, and all contain thinner bedded metasandstones with more abundant current markings than are found in other units of each area. On this basis, I conclude that the southern unit of Blue Mountain is potentially correlative with some part of units Trs2 and Trr in the Eugene Mountains (Fig. 5).

In evaluating potential correlations between Blue Mountain units and those in the Eugene Mountains, it is worth noting that the two areas are separated by only ~5 km and a high-angle Cenozoic normal fault on the southwest side of Blue Mountain (Fig. 4). The close proximity between the two areas supports the concept that correlations between units should be possible. The down-to-the-south sense of displacement on the southwest side of Blue Mountain dictates that contacts north of the fault should be located northwest of equivalent contacts south of the fault, which is consistent with the correlations shown in Figures 4 and 5.

It is also worth noting two other points in the context of the correlations proposed here. (1) They are internally consistent on a regional scale. Correlations based on comparisons with the Eugene Mountains imply that strata in Blue Mountain are overturned and that the oldest Blue Mountain unit (the northern unit) is late early or middle Norian in age, whereas the younger units are late Norian (Figs. 4–6). Likewise, correlations based on comparing units in Blue Mountain with those in the Santa Rosa Range and Bloody Run Hills also indicate that the Blue Mountain strata are overturned, that all these strata are Norian, and that the oldest Blue Mountain unit could be middle Norian in age (Fig. 5). The interpretation of overturned units in Blue Mountain is not unreasonable—all units in the Eugene Mountains are overturned, as are units in the hanging wall of the reverse fault in the western Santa Rosa Range (Fig. 6; Compton, 1960; Thole and Prihar, 1998; Rogers, 1999; Wyld et al., 2001). (2) Moving from northeast (San-

ta Rosa Range) to southwest (Eugene Mountains), there is an increasing abundance of carbonate interbeds in the Norian stratigraphic successions of the various areas, as well as an increasing abundance of feldspar in sandstones of the younger units (Fig. 5, Table 1). These variations imply progressive and systematic changes in depositional environment and provenance of sediments from north to south in this part of the basinal terrane.

## DEFORMATION OF TRIASSIC STRATA

Two phases of deformation are evident in Triassic strata of Blue Mountain. The first phase,  $D_1$ , was accompanied by low-grade regional metamorphism ( $M_1$ ), and produced the dominant structural grain within the Triassic strata. The second phase,  $D_2$ , is only locally developed and was not accompanied by metamorphism.

### $D_1$ Deformation and $M_1$ Metamorphism

Structures developed during the  $D_1$  phase of deformation include a pervasive cleavage ( $S_1$ ) and abundant folds of bedding ( $F_1$ ), as well as an inferred reverse fault (Fig. 3). The  $S_1$  cleavage is best developed in the metashales that constitute the majority of the Triassic section (Fig. 7). In these rocks,  $S_1$  is a continuous slaty to phyllitic cleavage defined primarily by aligned metamorphic muscovite and chlorite, as well as by slightly elongate quartz grains and seams of opaque material (Fig. 8A). In metasilstones,  $S_1$  is a closely spaced cleavage, and metasandstones exhibit either a flaggy spaced  $S_1$  cleavage or no evident cleavage. The  $S_1$  cleavage is very consistent in orientation throughout Blue Mountain, averaging  $N71^\circ E$  in strike and  $45^\circ NW$  in dip (Figs. 3 and 9).

A variety of features indicate that the  $S_1$  cleavage developed under low-grade metamorphic conditions. (1) The presence of abundant syntectonic white mica and chlorite in metapelites indicates subgreenschist- or lowergreenschist-grade conditions. (2) Metasilstones exhibit clear textural evidence for cleavage formation by pressure-solution processes (Fig. 8B), whereas quartz grains in metasandstones exhibit undulose extinction and minor subgrain development but little other evidence for crystal-plastic deformation (Fig. 8C). As summarized by Passchier and Trouw (1996), these combined microtextural features are indicative of low-grade metamorphism at syntectonic temperatures of probably  $<400^\circ C$ . (3) Illite-crystallinity analyses of slates



Figure 7. (A) View looking northeast at  $S_1$  cleavage in central unit slates of Blue Mountain. Grass for scale is ~10–15 cm tall. (B) View to the northeast of  $F_1$  fold of bedding in interlayered quartzite (lighter, more resistant beds) and slate (darker, more recessive beds) of central unit in Blue Mountain. Note axial-planar  $S_1$  cleavage in slates and hinge region of quartzite and asymmetry of folds indicating vergence to the southeast. Hammer for scale is ~30 cm long.

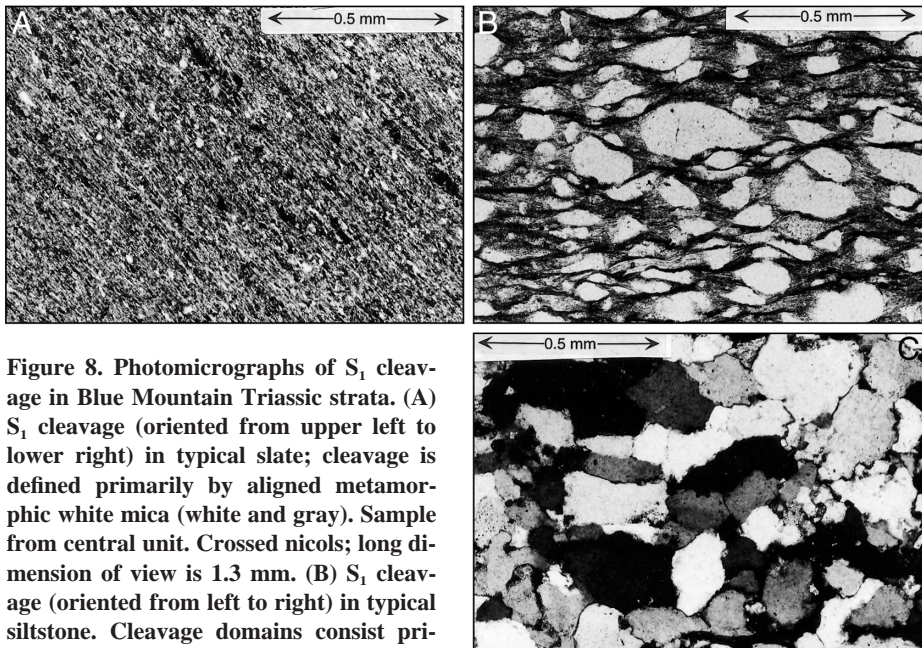


Figure 8. Photomicrographs of  $S_1$  cleavage in Blue Mountain Triassic strata. (A)  $S_1$  cleavage (oriented from upper left to lower right) in typical slate; cleavage is defined primarily by aligned metamorphic white mica (white and gray). Sample from central unit. Crossed nicols; long dimension of view is 1.3 mm. (B)  $S_1$  cleavage (oriented from left to right) in typical siltstone. Cleavage domains consist primarily of fine-grained opaque material, with some white mica and chlorite. Microlithon domains contain elongate quartz (white) and pressure shadows of fine-grained quartz and chlorite. Sample from central unit. Plane-polarized light; long dimension of view is 1.3 mm. (C) Typical quartzite from central unit. Note minor elongation of quartz grains and scarcity of subgrains or neocrystals, all of which point to minimal crystal-plastic deformation of quartz. Crossed nicols; long dimension of view is 1.3 mm.

and phyllites in Blue Mountain indicate that  $M_1$  metamorphism occurred under anchizone conditions (Rogers, 1999; Wyld et al., 2002).

The extent to which the  $S_1$  cleavage is developed in metasandstones is positively correlated with quartz and matrix content; thus, the more matrix-rich and quartz-poor metasandstones of the southern unit are commonly deformed by an  $S_1$  cleavage, the very pure quartzites of the central unit rarely have a

cleavage, and a variably developed cleavage is found in the intermediate-composition metasandstones of the northern unit. This positive correlation can be interpreted in the context of evidence that increasing clay (matrix) content in sedimentary rocks facilitates cleavage development (van der Pluijm and Marshak, 1997, p. 244–245) and that recrystallization of feldspar to fine-grained metamorphic phases (such as sericite, calcite, and quartz,

which partially replace feldspar grains in Blue Mountain sandstones) leads to reaction-enhanced ductility (e.g., White et al., 1980).

Macroscopic  $F_1$  folds of bedding are common in Triassic strata, and the  $S_1$  cleavage has an axial-planar orientation with respect to these folds (Figs. 3 and 7B). The folds vary in amplitude from ~15 cm to >50 m and are generally only evident when metasandstone beds are present to define a fold marker.  $F_1$  folds are mostly tight, although some are isoclinal, and they vary in shape from Ramsay class 1B or 1C (broadly parallel) in metasandstone beds to class 2 or 3 (broadly similar) with significant hinge thickening and limb thinning in slates and phyllites (Fig. 7B). Measured axial planes of  $F_1$  folds are similar in orientation to the  $S_1$  cleavage (Fig. 9). Measured fold axes are gently plunging and trend generally to the northeast, consistent with the orientation of the fold axis defined by the girdle distribution of bedding poles. Intersection lineations between  $S_1$  cleavage and bedding ( $L_{0 \times 1}$  lineations) have a similar orientation, consistent with the observation that  $S_1$  is axial planar to the folds (Figs. 7B and 9). Outcrop-scale folds are typically asymmetrical and generally have a vergence of top-up-to-the-southeast (Fig. 7B). Some folds, however, are symmetrical, and a few have a vergence of top-down-to-the-northwest. These relationships indicate that outcrop-scale folds are parasitic on even larger map-scale folds.

Quartz veins occur in some metasandstones and are interpreted to reflect brittle fracturing of these rocks during  $D_1$  deformation. This conclusion is based on the following: (1) The quartz veins occur only in metasandstone beds and do not penetrate into surrounding slates and phyllites. (2) The veins tend to be most abundant in the hinge regions of  $D_1$  folds. (3) The veins are present only in quartzites, not in feldspathic metasandstones, and they are prevalent only in the very pure quartzites of the central unit. This combination of features suggests that the pure quartzites behaved in a more brittle manner during  $D_1$  deformation than other rocks, resulting in abundant fractures, particularly in beds that were folded, and that these fractures were then filled by silica-rich metamorphic fluids that could have been derived from pressure-solution processes and metamorphic reactions in adjacent slates and phyllites. A similar correspondence between percent of quartz in metasandstones and presence or absence of abundant quartz veins is also observed in the Santa Rosa Range (Compton, 1960; Rogers, 1999).

$D_1$  deformation in Blue Mountain is also interpreted to have involved faulting of the

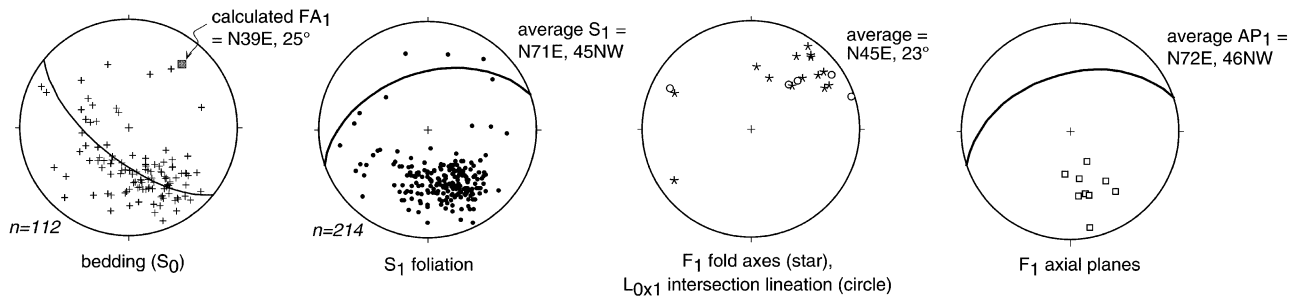


**Figure 9.** Lower-hemisphere equal-area projections of orientation data for  $D_1$  structures. Best-fit great circle and calculated  $F_1$  fold axis (FA) shown for bedding, AP—axial plane.

northern unit over the central unit (Figs. 3 and 6). This interpretation is based on the presence of several unusual structural and metamorphic features that are found only in the vicinity of the contact. (1) The regional  $S_1$  cleavage in metapelites is much more pronounced in the vicinity of the contact than it is elsewhere in the mountain; here metapelites break into leaf-thin sheets along  $S_1$  and may be best described as phyllonites, rather than slates or phyllites, in terms of their overall fabric. (2) Quartzite beds in the northern unit are extensively fractured and recrystallized near the contact, in contrast to quartzites farther from the contact. Both of these features suggest a localized increase in strain along the contact, consistent with fault displacement here. (3) There is an anomalous upgrading of the syntectonic  $M_1$  metamorphic assemblage in metapelites near the contact; here,  $S_1$  is locally defined by aligned biotite in addition to the usual muscovite and chlorite. This feature is particularly common in the phyllonitic rocks and requires some localized process along the contact that could facilitate or promote prograde metamorphic reactions. The most plausible explanation is that the contact is a fault along which there was enhanced fluid flow during  $M_1$  metamorphism and  $D_1$  deformation and that these fluids facilitated prograde metamorphic reactions. The only other alternative explanations for this feature are localized variations in protolith composition of metapelites near the contact or heating associated with a syntectonic intrusion emplaced in a localized zone along the contact; however, there is no supporting evidence in favor of either of these possibilities. Structure contouring of the fault indicates that it has an overall orientation of  $\sim N60^\circ E$ ,  $\sim 55^\circ NW$ , making it a reverse fault.

Collectively, the  $D_1$  structures just described provide evidence for significant northwest-southeast shortening in Triassic strata of Blue Mountain, with tectonic transport toward the southeast. An approximation of the minimum amount of shortening accom-

plished during  $D_1$  can be obtained by measuring the length of beds along folds between two points and comparing this length with the present distance between these two points as measured perpendicular to the axial planes of the folds. This analysis can only be done on metasandstone beds, because these are the only rocks in which macroscopic  $D_1$  folds are recognizable. Measurements of this type were made on 20 different folded beds, from locations throughout the mountain. These measurements consistently indicate shortening of 55%–75%. This range is considered a minimum because it does not take into account shortening associated with development of the  $S_1$  cleavage or reverse faulting.

## $D_2$ Deformation

$D_2$  deformation in Blue Mountain is only locally developed (Fig. 10); it involved formation of relatively open folds, crenulations, and a spaced cleavage that reorient or cut the older  $S_1$  fabric. The character of  $D_2$  structures varies with rock type. In slates and phyllites, the most common  $D_2$  structures are weak crenulation folds ( $F_{2c}$ ) of the  $S_1$  foliation. Rarely, the crenulation folds are associated with an axial-planar crenulation cleavage (Fig. 11A). More typically, the crenulations occur in rocks that are also cut by a spaced cleavage ( $S_2$ ) whose cleavage-domain spacing (3 mm to 2 cm) is greater than the spacing between crenulation-fold limbs ( $<3$  mm). Where metasandstone beds are present, larger  $F_2$  folds formed (Fig. 11B) and are locally associated with an axial-planar spaced  $S_2$  cleavage similar to that seen in slates and phyllites. The larger folds are mostly open in interlimb angle less commonly closed; are parallel (class 1B); are commonly asymmetric with vergence to the northeast; and generally have a wavelength of 1 m to several meters (Fig. 11B).

In thin section, the  $S_2$  cleavage in slates and phyllites is defined by domains that are relatively enriched in opaque material and improv-

erished in quartz, suggesting that the dominant process of cleavage formation was pressure solution (Fig. 11A). No metamorphic mineral growth is associated with the  $S_2$  cleavage.  $D_2$  deformation thus took place under lower-temperature, more brittle conditions compared to  $D_1$ .

The orientation of  $D_2$  structures is shown in Figure 10; these structures are substantially different in orientation from those formed during  $D_1$ . Crenulation axes and the axes of larger  $F_2$  folds generally plunge moderately to the northwest.  $F_2$  axial planes strike northwest and dip steeply to the southwest, similar to the orientation of most  $S_2$  cleavage. Intersection lineations between the  $S_1$  and  $S_2$  cleavages ( $L_{1 \times 2}$  lineations) have an orientation similar to that of  $F_2$  fold axes, consistent with the observation that  $S_2$  is locally axial planar to these folds.

Collectively, the relationships described indicate that  $D_2$  deformation in Blue Mountain reflects northeast-southwest shortening via folding and minor cleavage development under low-temperature, nonmetamorphic conditions. The total amount of shortening associated with  $D_2$  deformation is minor—initial versus final length measurements on 10 folds indicate shortening of  $\sim 8\%$ – $25\%$ , but this is a maximum because  $D_2$  structures are only locally developed in Blue Mountain, are not pervasive where they occur, and often reflect heterogeneous strain (Figs. 10 and 11). A more realistic estimate of overall shortening associated with  $D_2$  is probably  $\leq 5\%$ .

## Megascopic Structure of Blue Mountain

The megascopic structure of Blue Mountain, defined by the stratigraphic and structural relationships already discussed, is one in which the oldest (northern) unit is faulted over the younger (central and southern) units, and in which the two younger units are overturned (Figs. 3 and 6). Overturning of the central and southern units implies that they are located on

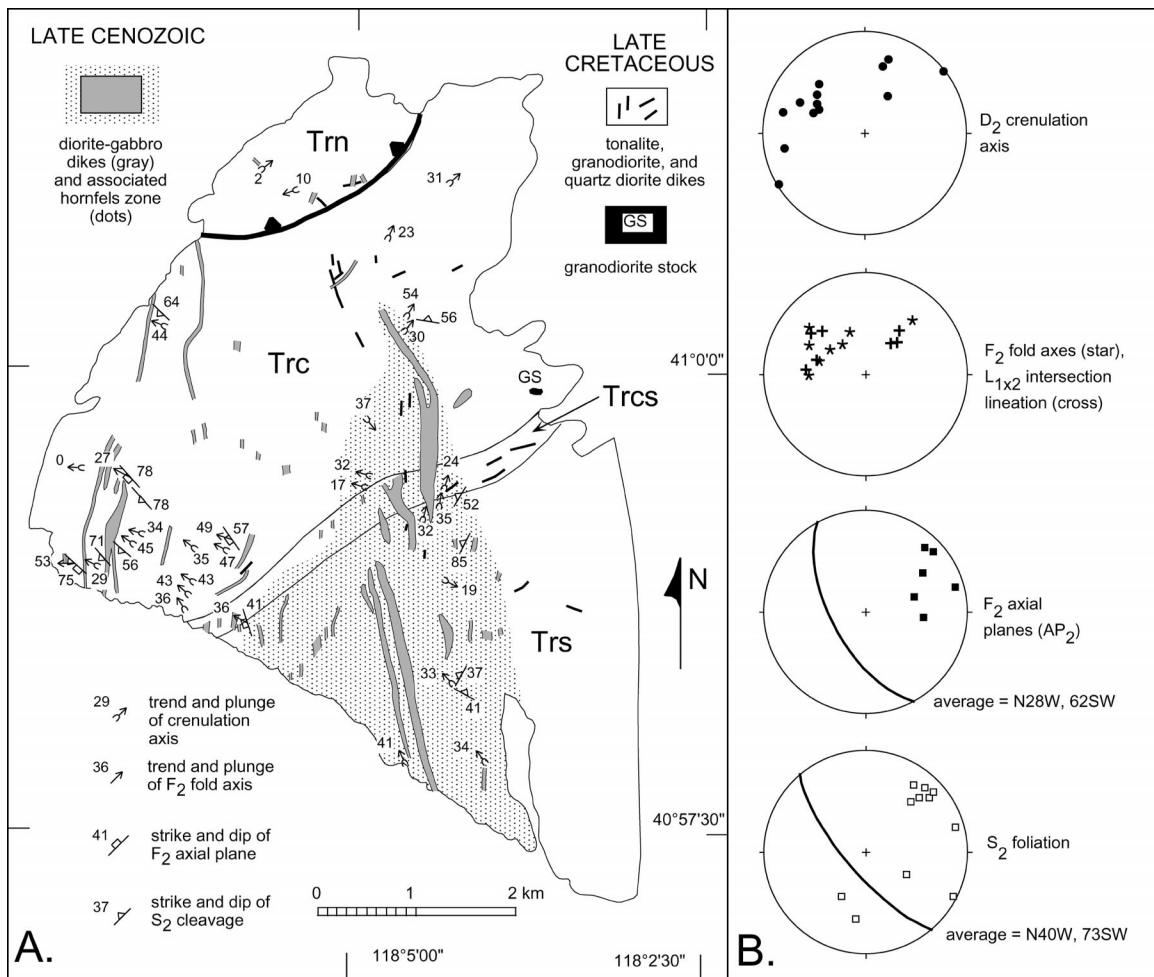


Figure 10. (A) Map of Blue Mountain showing location, character, and orientation of D<sub>2</sub> structures, location of posttectonic intrusions, and area of contact metamorphism associated with mafic dikes. Symbols same as in Figure 3. Thickness of thinner dikes exaggerated for clarity. Where dike ends are shown without a closed boundary, they were not mapped beyond where they are shown. (B) Lower-hemisphere equal-area projections of orientation data for D<sub>2</sub> structures.

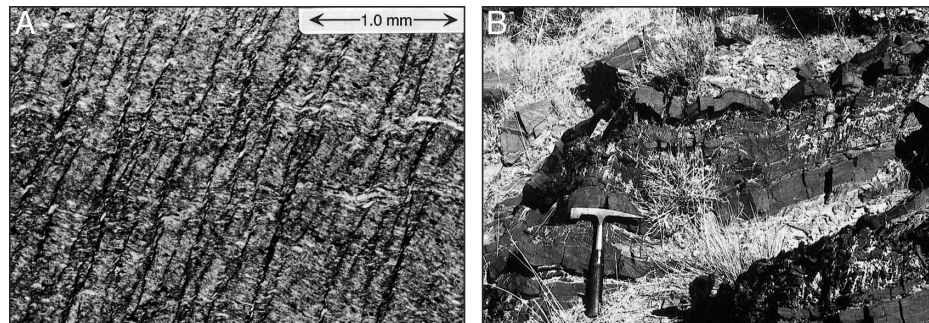


Figure 11. (A) Photomicrograph of D<sub>2</sub> crenulation cleavage in slate of central unit. S<sub>1</sub> cleavage oriented from left to right. S<sub>2c</sub> cleavage oriented from upper right to lower left and defined by seams of opaque material. Plane-polarized light; long dimension of view is 3.2 mm. (B) View to northwest of F<sub>2</sub> fold of bedding and S<sub>1</sub> cleavage in central unit. Hammer for scale is ~30 cm long.

the western limb of an overturned megascopic syncline whose hinge region is to the south-east of Blue Mountain and/or that they are on the eastern limb of an overturned megascopic anticline whose hinge region is cut out by the reverse fault in the northwest part of Blue Mountain. Further evidence for megascopic folding in this area can only be obtained through additional mapping east of Blue Mountain. It is relevant to note, however, that the presence of megascopic overturned folds in Blue Mountain is supported by the asymmetry and vergence relationships of macroscopic folds described earlier and that the megascopic structure of Blue Mountain defined by this study is quite similar to that in the Eugene Mountains and Santa Rosa Range (Figs. 4 and 6; Thole and Prihar, 1998; Wyld et al., 2001).

I interpret that megascopic folding and

overturning of units in Blue Mountain is related to  $D_1$  deformation, and not to  $D_2$ . This conclusion is based on the following: (1) The northeast strike and northwest dip of the central and southern units requires that they are on the limb of a large fold whose axial plane has a similar orientation; this is consistent with  $D_1$  deformation but inconsistent with  $D_2$ . (2) Large-scale folding and overturning of units imply major shortening, which is consistent with  $D_1$  deformation but inconsistent with  $D_2$ .

## POSTTECTONIC INTRUSIONS

Two suites of posttectonic intrusions occur in Blue Mountain, an older suite of felsic intrusions that are minor in abundance and a younger suite of mafic dikes that form a prominent north-trending dike swarm (Figs. 3 and 10A). The older felsic suite occurs mostly in the eastern half of Blue Mountain and includes small, discontinuous dikes (30 cm to 2 m wide) and one small stock (Fig. 10A). Compositions of these intrusions are mostly tonalite, with lesser granodiorite and quartz diorite. Generally, ~5% phenocrysts are present, including some combination of hornblende (now replaced by chlorite and calcite), plagioclase, and biotite. The felsic intrusions post-date  $D_1$  deformation because they do not exhibit any evidence for solid-state strain, they locally cut the  $S_1$  cleavage in slates and phyllites, and they locally contain xenoliths of slate and phyllite. No crosscutting relationships between the felsic intrusions and  $D_2$  structures have been observed, so the timing of this phase of intrusion relative to  $D_2$  deformation is unknown.

Although undated, there are two lines of evidence suggesting that the felsic intrusions are of Late Cretaceous age. (1)  $^{40}\text{Ar}/^{39}\text{Ar}$  whole-rock analyses of slates and phyllites in Blue Mountain indicate that these rocks underwent two periods of Ar loss after regional deformation, both of which are best explained in terms of thermal effects associated with emplacement of local intrusions and the first of which occurred at ca. 85 Ma (Wyld et al., 1999, 2002). (2) The Eugene Mountains, directly to the south (Fig. 4), contain an abundance of similar felsic intrusions, including granodioritic plutons and stocks, and numerous granodioritic, andesitic, and aplitic dikes (Fig. 6), which have been dated at 89–68 Ma (K-Ar on biotite; Thole and Prihar, 1998), similar to the time of Cretaceous Ar loss in slates and phyllites of Blue Mountain.

The mafic dikes of Blue Mountain form a north-trending swarm that is concentrated in

the western two thirds of the area; the largest dikes are along the southeast side of the swarm (Figs. 3 and 10A). The dikes have a subvertical dip (Fig. 6) and range in thickness from ~1 m to ~200 m, although most are <30 m thick. Compositions vary from pyroxene diorite or gabbro (most common) to pyroxene quartz diorite.

The mafic dikes cut directly across bedding, unit contacts, and  $D_1$  structures in Triassic strata (Fig. 3) and also locally cut across the felsic dikes (Fig. 10A). Thermal metamorphism and recrystallization of the Triassic wall rocks is evident immediately adjacent to the dike margins, as well as in a wider zone surrounding the bigger dikes (Fig. 10A). Within this zone, the  $S_1$  cleavage is still visible in metashales but is overprinted by very fine grained crosscutting minerals that impart a weak hornfels texture to the rocks. Crosscutting minerals in the hornfels zone include muscovite, chlorite, zoisite/clinozoisite, and/or biotite. Where the  $S_2$  crenulation cleavage is present in the Triassic strata of the hornfels zone, it is also crosscut by the contact-metamorphic minerals. The dikes are interpreted to be late Tertiary on the basis of the ca. 10 Ma age of the second episode of Ar loss reflected in the  $^{40}\text{Ar}/^{39}\text{Ar}$  analyses of slates and phyllites from Blue Mountain (Wyld et al., 1999, 2002).

## REGIONAL STRUCTURAL CORRELATIONS

Structural relationships in Blue Mountain can be compared with those defined in nearby areas to clarify the regional structural development of the northern Luning-Fencemaker fold-and-thrust belt. Nearby areas for which there are structural data are the Jungo area to the west (Folsom, 2000; Wyld, 2000; Wyld et al., 2002), the Eugene Mountains to the south (Thole and Prihar, 1998), and the Krum Hills (Martin, 1999), northern East Range (Elison and Speed, 1989), and southern Santa Rosa Range (Rogers, 1999; Wyld et al., 2001) to the east and northeast (Fig. 2). Critical comparative structural relationships between these areas and Blue Mountain are listed in Table 2 and summarized next.

### $D_1$ Deformation

All of the areas listed in Table 2 contain evidence for a major  $D_1$  phase of deformation that produced a dominant northeast-trending, northwest-dipping structural grain in Triassic rocks.  $D_1$  structures are very similar in all the areas and include a prominent  $S_1$  cleavage that

is continuous in metapelites and generally spaced in metasandstones, abundant tight to isoclinal  $F_1$  folds of bedding, and thrust or reverse faults that place older basinal-terrace units over younger units to the southeast. The scale of  $F_1$  folding varies from macroscopic (common in all areas) to megascopic—with wavelengths of hundreds to thousands of meters. Megascopic folds are defined by the outcrop pattern of Triassic units in the Santa Rosa Range, the northern East Range, and the Jungo area, and can be inferred from the overturning of Triassic units in Blue Mountain and the Eugene Mountains (Fig. 6). Orientation of  $D_1$  structures and asymmetry of folds consistently indicate northwest-southeast shortening and tectonic transport to the southeast. In all areas where amount of shortening has been calculated,  $D_1$  deformation accommodated substantial shortening, with minimum estimates ranging from 50% to 75%. All across the northern Luning-Fencemaker fold-and-thrust belt,  $D_1$  deformation was accompanied by regional, low-grade metamorphism (Table 2). Where studied in detail (Jungo area, Blue Mountain, Santa Rosa Range), the grade of metamorphism achieved was anchizone to epizone (Rogers, 1999; Wyld et al., 1999, 2002), equivalent to the subgreenschist to lower-greenschist grade in metabasaltic rocks (Kisch, 1987).

It is reasonable to conclude, on the basis of the relationships summarized previously in this paper, that  $D_1$  structures in all the various areas listed in Table 2 are the result of a single deformational event that affected the entire province. The timing of  $D_1$  deformation in the various areas is not precisely defined, and it is unclear whether there is a variation in the timing of this deformation across the province. In all areas listed in Table 2, an older age limit for deformation is defined by the latest Triassic age of the youngest deformed rocks. Posttectonic granitic intrusions (Figs. 2 and 4) provide an upper age constraint of 102–85 Ma (middle Cretaceous) in many of the areas. Undeformed and unmetamorphosed Cretaceous alluvial strata overlie deformed Triassic rocks along a major angular unconformity in the Krum Hills, just east of Blue Mountain (Fig. 4), and provide a somewhat older upper age constraint of 125–123 Ma for  $D_1$  deformation in this area based on the age of these strata (Quinn et al., 1997; Martin, 1999). Finally,  $^{40}\text{Ar}/^{39}\text{Ar}$  whole-rock dating of slates and phyllites from the southern Santa Rosa Range, Blue Mountain, and the Jungo area indicates that  $D_1$  deformation in these rocks occurred prior to 145–140 Ma, and probably significantly prior to this time, po-

TABLE 2. DEFORMATION PHASES IN THE NORTHERN LUNING-FENCEMAKER FOLD-AND-THRUST BELT

Blue Mountain (this paper; Wyld et al., 2002)	Jungo area (Folsom, 2000; Wyld, 2000; Wyld et al., 2002)	Eugene Mountains (Thole and Prihar, 1998)	Krum Hills (Quinn et al., 1997; Martin, 1999)	Northern East Range (Elison and Speed, 1989; Elison, 1995)	Santa Rosa Range (Rogers, 1999; Wyld et al., 2001)
<u>D<sub>1</sub> deformation</u> Pervasive cleavage, tight to isoclinal folds, reverse fault Low-grade metamorphism 55%–75% NW-SE shortening SE tectonic transport Predates ca. 85 Ma intrusions	<u>D<sub>1</sub> deformation</u> Pervasive cleavage, tight to isoclinal folds, thrust faults Low-grade metamorphism 60%–75% NW-SE shortening SE tectonic transport Predates 101–97 Ma intrusions	<u>D<sub>1</sub> deformation</u> Pervasive cleavage, tight to isoclinal folds, thrust faults Low-grade metamorphism NW-SE shortening SE tectonic transport Predates 89–68 Ma intrusions	<u>D<sub>1</sub> deformation</u> Pervasive cleavage Low-grade metamorphism NW-SE shortening Predates deposition of King Lear Formation alluvial strata at ca 125– 123 Ma	<u>D<sub>1</sub> deformation</u> Pervasive cleavage, tight folds, thrust faults Low-grade metamorphism 50%–70% NW-SE shortening SE tectonic transport	<u>D<sub>1</sub> deformation</u> Pervasive cleavage, tight to isoclinal folds, reverse fault Low-grade metamorphism 55%–70% NW-SE shortening SE tectonic transport Predates 102 Ma intrusion
No equivalent deformation present	No equivalent deformation present	No equivalent deformation present	No equivalent deformation present	<u>D<sub>2</sub> deformation</u> Locally developed Open folds, local spaced cleavage, reverse faults Minor NW-SE shortening SE tectonic transport Predates 153 Ma intrusion	<u>D<sub>2</sub> deformation</u> Locally developed Open to closed folds, local spaced cleavage Minor NW-SE shortening SE tectonic transport Predates 102 Ma intrusion
No equivalent deformation present	No equivalent deformation present	No equivalent deformation present	No equivalent deformation present	No equivalent deformation present	<u>D<sub>3</sub> deformation</u> Minor subvertical shortening
<u>D<sub>2</sub> deformation</u> Locally developed Crenulations and open to closed folds, minor spaced cleavage Minor NE-SW shortening Predates ca. 10 Ma dikes	<u>D<sub>2</sub> deformation</u> Locally developed Crenulations and open to closed folds, minor spaced cleavage Minor NE-SW shortening	<u>D<sub>2</sub> deformation</u> Locally developed Open folds, reverse faults Minor shortening Related(?) to emplacement of 89–68 Ma intrusions	No equivalent deformation observed	<u>D<sub>2</sub> deformation</u> Locally developed Folds, foliation Minor NE-SW shortening	<u>D<sub>2</sub> deformation</u> Locally developed Crenulations and open to closed folds, minor spaced cleavage Minor NE-SW shortening Syntectonic with 102 Ma intrusion

Note: Inferred correlative phases of deformation are shown in same rows, although numbering of different phases varies with area.

tentially in the late Early Jurassic (Wyld and Wright, 2000; Wyld et al., 1999, 2002). On a more regional scale, the youngest dated strata in the northern Luning-Fencemaker fold-and-thrust belt that were deformed by structures similar to D<sub>1</sub> are Lower Jurassic (as young as middle Toarcian) sedimentary rocks in the west Humboldt Range (Fig. 2), and these are intruded by a posttectonic pluton dated at 165 Ma by U-Pb zircon (Speed, 1974; Wyld and Wright, 2000). Collectively, these data indicate that D<sub>1</sub> deformation in the northern Luning-Fencemaker fold-and-thrust belt occurred in the Jurassic, probably in the late Early to Middle Jurassic.

#### Younger Northwest-Southeast Shortening

Two of the areas listed in Table 2 (Santa Rosa Range and northern East Range) were affected by a second phase of northwest-southeast shortening, whereas the rest of the areas, including Blue Mountain, were not. Structures formed during this younger northwest-southeast shortening event in the Santa Rosa Range and northern East Range (referred to as D<sub>2</sub> in both areas) include open to closed folds, reverse faults, and a locally developed spaced cleavage (Table 2). Cross-cutting relationships in the Santa Rosa Range

indicate that this phase of deformation predates emplacement of middle Cretaceous granitic intrusions at 102–100 Ma (Smith et al., 1971; Wyld et al., 2001), whereas in the northern East Range, this phase of deformation is said to predate intrusion of a pluton dated at ca. 153 Ma (Elison and Speed, 1989; Elison, 1995). The second phase of northwest-southeast shortening therefore appears to have occurred in the Jurassic.

Elison and Speed (1989), Rogers (1999), and Wyld et al. (2001) used local structural relationships in their respective field areas to argue that the second phase of northwest-southeast shortening in the northern East Range and Santa Rosa Range was associated with final emplacement of basinal strata over coeval shelf rocks along the Fencemaker thrust, which is located just east of the Santa Rosa Range and within the northern East Range (Fig. 2). This conclusion is further supported by the data presented in this paper and in Table 2 indicating that areas farther west of the Fencemaker thrust (Blue Mountain, Eugene Mountains, and Jungo area; Fig. 2) were not affected by a second phase of northwest-southeast shortening. It therefore appears that structural effects associated with emplacement of the Fencemaker thrust did not extend far from the fault.

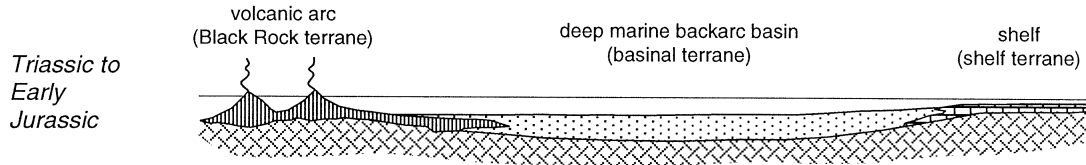
#### Subvertical Shortening

A phase of subvertical shortening is recognized in the Santa Rosa Range (where it is referred to as D<sub>3</sub>) but nowhere else in the northern Luning-Fencemaker fold-and-thrust belt (Table 2; Wyld et al., 2001). This phase of deformation produced broad warps of older structures about megascopic folds with sub-horizontal axial planes (Table 2), and is interpreted to reflect minor subvertical shortening associated with initial emplacement of Cretaceous plutons in this area (Rogers, 1999; Wyld et al., 2001). This deformation is clearly not of any regional structural significance and it will not be considered here any further.

#### Late-Phase Northeast-Southwest Shortening

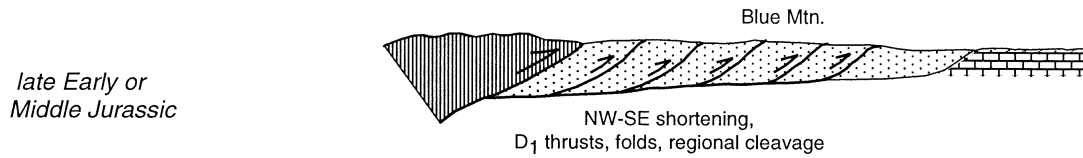
The youngest phase of shortening deformation documented in all the areas listed in Table 2 shares obvious similarities, suggesting that this represents a second regional deformation event that affected the entire northern Luning-Fencemaker fold-and-thrust belt. Numerical notation assigned to this last phase of shortening varies with area, depending on the number of prior local deformational events; thus, it is referred to as D<sub>2</sub> in Blue Mountain,

### A. ACCUMULATION OF BASINAL TERRANE CLASTICS IN BACKARC BASIN



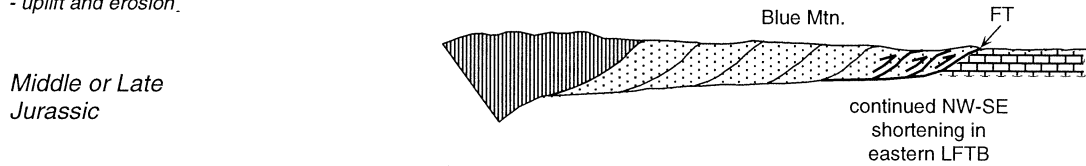
### B. D<sub>1</sub> DEFORMATION IN LFTB

- main structural closure of backarc basin; major crustal shortening and thickening
- structural burial of basinal terrane strata leads to M<sub>1</sub> metamorphism

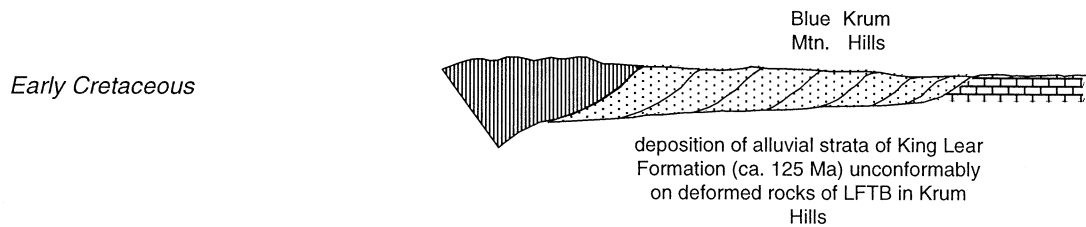


### C. LATE PHASE DEFORMATION IN LFTB

- restricted to eastern LFTB and related to final emplacement of basinal strata over shelf along Fencemaker thrust (FT)
- structural closure of backarc basin completed
- uplift and erosion.



### D. TECTONIC QUIESCENCE, SUBAERIAL EXPOSURE



### E. PLUTONISM, SEVIER OROGENY, AND SYNPLUTONIC DEFORMATION

- minor NE-SW shortening
- locally-developed, heterogeneous strain

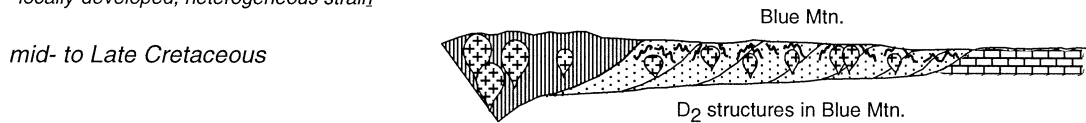


Figure 12. Schematic model of the evolution of the northern basinal terrane and Luning-Fencemaker fold-and-thrust belt from the Triassic to Late Cretaceous. No specific scale is implied.

the Jungo area, and the Eugene Mountains, as D<sub>3</sub> in the northern East Range, and as D<sub>4</sub> in the Santa Rosa Range (Table 2).

In all areas where detailed structural information is available (Santa Rosa Range, Blue Mountain, Jungo area, and northern East

Range), the last phase of shortening deformation is characterized by the following: Structures include open folds and crenulations plus a spaced or crenulation cleavage; these structures are only locally developed and reflect heterogeneously distributed strain; folds

and cleavage reflect northeast-southwest shortening, nearly orthogonal to those associated with D<sub>1</sub> deformation; and the total amount of shortening associated with the late-phase deformation, based on bed-length measurements of folded layers and the heteroge-

neous distribution of structures, is minimal (Table 2). These data lead me to conclude that late-phase shortening structures in Blue Mountain, the Jungo area, the Santa Rosa Range, and the northern East Range were all produced during the same northeast-southwest shortening event. The timing of the late-phase northeast-southwest shortening event is precisely defined only in the Santa Rosa Range (Rogers, 1999; Wyld et al., 2001). Here, late-phase ( $D_4$ ) structures increase in strain and syntectonic metamorphic grade in the thermal aureole of a stock dated at 102 Ma, indicating that this deformation is middle Cretaceous.

The youngest phase of shortening deformation in the Eugene Mountains is not described in much detail (Thole and Prihar, 1998), making comparisons with other areas somewhat tenuous. I suggest a correlation with late-phase deformation in the other areas, however, for the following reasons: (1) The late-phase deformation in the Eugene Mountains is similar to that in other areas in that it produced only locally developed structures, including open folds with little or no associated cleavage, that accommodated minimal shortening (Table 2). (2) Thole and Prihar (1998) have argued that late-phase structures in the Eugene Mountains formed during intrusion of middle to Late Cretaceous stocks, which is consistent with the age constraints and synplutonic relationships of late-phase structures in the Santa Rosa Range (Wyld et al., 2001).

## INTERPRETATION AND DISCUSSION

The picture that emerges from this study is that a clear sequence of events and processes affected the northern Luning-Fencemaker fold-and-thrust belt during the Mesozoic. This sequence is depicted schematically in Figure 12.

The Late Triassic, in this part of the Cordillera, was characterized by deposition of deep-marine clastic strata in a basin situated between the continental shelf and an offshore volcanic arc (Fig. 12A). Strata in Blue Mountain are typical of the basinal terrane: mudstone dominates, forming ~80% of the Triassic succession, and the remainder consists of siltstone (10%), quartz-rich sandstone (~10%), and rare carbonate. As elsewhere in the basinal terrane, the thickness of the Triassic succession in Blue Mountain is large: total structural thickness is ~6700 m.

Deformation of the backarc basin primarily occurred during a single  $D_1$  event that affected the entire northern basinal terrane, accommodated substantial northwest-southeast short-

ening, and resulted in development of a ductile fold-and-thrust belt with consistent structural vergence to the southeast (Fig. 12B). Available evidence indicates that this  $D_1$  deformation occurred in the late Early and/or Middle Jurassic, which is similar to the time frame when major orogenesis affected the arc provinces to the west (Fig. 1; Burchfiel et al., 1992). It is clear that the principal structural architecture of the northern Luning-Fencemaker fold-and-thrust belt developed during the  $D_1$  deformation, and it is reasonable to conclude that it was this deformational phase that led largely or entirely to structural closure of the backarc basin (Fig. 12B). Polyphase northwest-southeast shortening during continued development of the fold-and-thrust belt is confined to the eastern part of the province, near the Fencemaker thrust, and did not affect areas farther to the west like Blue Mountain (Fig. 12C).

One particularly interesting outcome of the analysis in this study is the evidence that the megascopic structure of several areas along strike from one another in the northern Luning-Fencemaker fold-and-thrust belt is quite similar. Specifically, the Santa Rosa Range, Blue Mountain, and the Eugene Mountains all have (1) a megascopic structure involving a  $D_1$  reverse fault to the northwest, and (2) strata that are either known or likely to be deformed by megascopic overturned  $D_1$  folds in the footwall of the fault (Figs. 4 and 6). It is possible that, with further mapping in the intervening areas, these megascopic structures could be definitively correlated along strike. At a minimum, it is apparent that major folds and faults can likely be identified and correlated on a regional scale in the Luning-Fencemaker fold-and-thrust belt, much as they are in other fold-and-thrust belts of the world. Additional information of this type on regional structures in the Luning-Fencemaker belt would add considerably to our understanding of the structural character and development of this backarc fold-and-thrust belt.

Following the Jurassic northwest-southeast shortening, a period of tectonic quiescence characterized the northern Luning-Fencemaker belt (Fig. 12D). During this period, which apparently spanned much of the Early Cretaceous and possibly part of the Late Jurassic, there is no evidence of any deformation in the northern belt. Instead, the province appears to have been characterized by exhumation and erosion during this time frame, on the basis of relationships in the Krum Hills, just east of Blue Mountain (Fig. 12D). Additional support for this interpretation is the fact that younger Cretaceous deformation in the region gener-

ally occurred under lower-temperature, non-metamorphic conditions, in contrast with the earlier, synmetamorphic Jurassic deformation (Table 2).

Subsequent deformation in the northern Luning-Fencemaker fold-and-thrust belt accommodated relatively minor shortening and occurred in the middle to Late Cretaceous, during the same time frame when Cretaceous granitic intrusions were emplaced into the backarc region (Fig. 12E). This late-stage deformation cannot be considered a manifestation of continued development of the fold-and-thrust belt as a structural province: The late-stage deformation reflects a very different shortening direction from that in the Jurassic; it nowhere resulted in the formation of a fold-and-thrust complex; and it was separated from the Jurassic deformation by a lengthy period of tectonic quiescence, exhumation, and erosion (Fig. 12). Late-stage deformation in the Luning-Fencemaker belt is instead most likely related to the Sevier orogeny and event that culminated with development of the Sevier fold-and-thrust belt farther to the east (Fig. 1) in the middle to Late Cretaceous (Armstrong, 1968; Lawton, 1985; Heller et al., 1986).

## ACKNOWLEDGMENTS

This research was supported by the National Science Foundation grant EAR-9796174. I gratefully acknowledge the assistance of Jill Weinberger, who acted as my field assistant during the mapping of Blue Mountain. The research and paper have benefited from discussions with Johannah Rogers, Heather Folsom, Peter Copeland, James E. Wright, John Oldow, and William R. Dickinson, and the final version of the manuscript benefited from reviews by Calvin H. Stevens, John S. Oldow, and J. Douglas Walker.

## REFERENCES CITED

- Armstrong, R.L., 1968, Sevier orogenic belt in Nevada and Utah: *Geological Society of America Bulletin*, v. 79, p. 429–458.
- Burchfiel, B.C., Cowan, D.S., and Davis, G.A., 1992, Tectonic overview of the Cordilleran orogen in the western United States, in Burchfiel, B.C., Lipman, P.W., and Zoback, M.L., eds., *The Cordilleran orogen: Continuous U.S.: Boulder, Colorado, Geological Society of America, Geology of North America*, v. G-3, p. 407–479.
- Compton, R.R., 1960, Contact metamorphism in the Santa Rosa Range, Nevada: *Geological Society of America Bulletin*, v. 71, p. 1383–1416.
- Elison, M.W., 1995, Causes and consequences of Jurassic magmatism in the northern Great Basin: Implications for tectonic development, in Miller, D.M., et al., eds., *Jurassic magmatism and tectonics of the North American Cordillera: Geological Society of America Special Paper 299*, p. 249–266.
- Elison, M.W., and Speed, R.C., 1989, Structural development during flysch basin collapse: The Fencemaker allochthon, East Range, Nevada: *Journal of Structural Geology*, v. 11, p. 523–538.
- Folsom, H.K., 2000, Analysis of Mesozoic deformation in

- a backarc basin, northwestern Nevada [senior honor's thesis]: Athens, University of Georgia, 92 p.
- Gehrels, G.E., and Dickinson, W.R., 1995, Detrital zircon geochronology of Neoproterozoic to Triassic miogeoclinal and eugeoclinal strata in Nevada: *American Journal of Science*, v. 295, p. 18–48.
- Heller, P.L., Bowdler, S.S., Chambers, H.P., Coogan, J.C., Hagen, E.S., Shuster, M.W., Winslow, N.S., and Lawton, T.F., 1986, Time of initial thrusting in the Sevier orogenic belt, Idaho-Wyoming and Utah: *Geology*, v. 14, p. 388–391.
- Johnson, M.G., 1977, Geology and mineral deposits of Pershing County, Nevada: Nevada Bureau of Mines and Geology Bulletin 89, 115 p.
- Kisch, H.J., 1987, Correlation between indicators of very-low-grade metamorphism, in Frey, M., ed., *Low temperature metamorphism*: Glasgow, Blackie and Son, p. 227–300.
- Lawton, T.F., 1985, Style and timing of frontal structures, thrust belt, central Utah: *American Association of Petroleum Geologist Bulletin*, v. 69, p. 1145–1159.
- Lupe, R., and Silberling, N.J., 1985, Genetic relationship between lower Mesozoic continental strata of the Colorado Plateau and marine strata of the Western Great Basin: Significance for accretionary history of Cordilleran lithotectonic terranes, in Howell, D.G., ed., *Tectonostratigraphic terranes of the circum-Pacific region*: Houston, Circum-Pacific Council for Energy and Mineral Resources, Earth Science Series 1, p. 263–270.
- Manuszak, J.D., Satterfield, J.I., and Gehrels, G.E., 2000, Detrital zircon geochronology of Upper Triassic strata in western Nevada, in Soreghan, M.J., and G.E., Gehrels, eds., *Paleozoic and Triassic paleogeography and tectonics of western Nevada and northern California*: Geological Society of America Special Paper 347, p. 109–118.
- Martin, A.J., 1999, Stratigraphy and tectonic setting of the Lower Cretaceous King Lear Formation, Jackson Mountains, northwest Nevada [M.Sc. thesis]: Houston, Rice University, 84 p.
- Nichols, K.M., and Silberling, N.J., 1977, Stratigraphy and depositional history of the Star Peak Group (Triassic), northwestern Nevada: *Geological Society of America, Special Paper 178*, 73 p.
- Oldow, J.S., 1978, Triassic Pamlico Formation: An allochthonous sequence of volcanogenic-carbonate rocks in west-central Nevada, in Howell, D.G., and McDougall, K.A., eds., *Mesozoic paleogeography of the western U.S.*: Pacific Section, Society of Economic Paleontologists and Mineralogists, Pacific Coast Paleogeography Symposium 2, p. 223–236.
- Oldow, J.S., 1984, Evolution of a late Mesozoic back-arc fold and thrust belt, northwestern Great Basin, U.S.A.: *Tectonophysics*, v. 102, p. 245–274.
- Oldow, J.S., Bartel, R.L., and Gelber, A.W., 1990, Depositional setting and regional relationships of basinal assemblages: Pershing Ridge Group and Fencemaker Canyon sequence in northwestern Nevada: *Geological Society of America Bulletin*, v. 102, p. 193–222.
- Passchier, C.W., and Trouw, R.A.J., 1996, *Microtectonics*: Berlin, Springer-Verlag, 289 p.
- Quinn, M.J., 1996, Pre-Tertiary stratigraphy, magmatism, and structural history of the central Jackson Mountains, Humboldt County, Nevada [Ph.D. thesis]: Houston, Rice University, 243 p.
- Quinn, M.J., Wright, J.E., and Wyld, S.J., 1997, Happy Creek igneous complex and tectonic evolution of the early Mesozoic arc in the Jackson Mountains, northwest Nevada: *Geological Society of America Bulletin*, v. 109, p. 461–482.
- Rogers, J.W., 1999, Jurassic–Cretaceous deformation in the Santa Rosa Range, Nevada: Implications for the development of the northern Luning-Fencemaker fold-and-thrust belt [M.Sc. thesis]: Athens, University of Georgia, 195 p.
- Smith, D.L., Wyld, S.J., Wright, J.E., and Miller, E.L., 1993, Progression and timing of Mesozoic crustal shortening in the northern Great Basin, western U.S.A., in Dunne, G., and McDougall, K., eds., *Mesozoic paleogeography of the western United States—II*: Los Angeles, Pacific Section, Society of Economic Paleontologists and Mineralogists, Book 71, p. 389–406.
- Smith, J.G., McKee, E.H., Tatlock, D.B., and Marvin, R.F., 1971, Mesozoic granitic rocks in northwest Nevada: A link between the Sierra Nevada and Idaho batholiths: *Geological Society of America Bulletin*, v. 82, p. 2933–2944.
- Speed, R.C., 1974, Evaporite-carbonate rocks of the Jurassic Lovelock Formation, west Humboldt Range, Nevada: *Geological Society of America Bulletin*, v. 85, p. 105–118.
- Speed, R.C., 1978a, Paleogeographic and plate tectonic evolution of the early Mesozoic marine province of the western Great Basin, in Howell, D.G., and McDougall, K.A., eds., *Mesozoic paleogeography of the western U.S.*: Los Angeles, Pacific Section, Society of Economic Paleontologists and Mineralogists, Pacific Coast Paleogeography Symposium 2, p. 253–270.
- Speed, R.C., 1978b, Basinal terrane of the early Mesozoic marine province of the western Great Basin, in Howell, D.G., and McDougall, K.A., eds., *Mesozoic paleogeography of the western U.S.*: Los Angeles, Pacific Section, Society of Economic Paleontologists and Mineralogists, Pacific Coast Paleogeography Symposium 2, p. 237–252.
- Speed, R.C., and Jones, T.A., 1969, Synorogenic quartz sandstone in the Jurassic mobile belt of western Nevada: Boyer Ranch Formation: *Geological Society of America Bulletin*, v. 80, p. 2551–2584.
- Thole, R.H., and Prihar, D.W., 1998, Geologic map of the Eugene Mountains, northwestern Nevada: Nevada Bureau of Mines and Geology Map 115, scale 1:24000, 1 sheet, 12 p.
- van der Pluijm, B.A., and Marshak, S., 1997, *Earth structure, An introduction to structural geology and tectonics*: WCB/McGraw-Hill, 495 p.
- White, S.H., Burrows, S.E., Carreras, J., Shaw, N.D., and Humphreys, F.J., 1980, On mylonites in ductile shear zones: *Journal of Structural Geology*, v. 2, p. 175–187.
- Willden, R., 1964, Geology and mineral deposits of Humboldt County, Nevada: Nevada Bureau of Mines Bulletin, v. 59, 154 p.
- Wyld, S.J., 1996, Early Jurassic deformation in the Pine Forest Range, northwest Nevada, and implications for Cordilleran tectonics: *Tectonics*, v. 15, p. 566–583.
- Wyld, S.J., 1998, Structural development of the Luning-Fencemaker fold-and-thrust belt: New constraints from northern Nevada: *Geological Society of America Abstracts with Programs*, v. 30, no. 5, p. 71.
- Wyld, S.J., 2000, Triassic evolution of the arc and back-arc of northwest Nevada, and evidence for extensional tectonism, in Soreghan, M.J., and G.E., Gehrels, eds., *Paleozoic and Triassic paleogeography and tectonics of western Nevada and northern California*: Geological Society of America Special Paper 347, p. 185–207.
- Wyld, S.J., and Wright, J.E., 2000, Timing of deformation in the Mesozoic Luning-Fencemaker fold-thrust belt, Nevada: *Geological Society of America Abstracts with Programs*, v. 32, no. 7, p. A169–A170.
- Wyld, S.J., Copeland, P., and Rogers, J.W., 1999,  $^{40}\text{Ar}/^{39}\text{Ar}$  whole rock phyllite ages from the Mesozoic Luning-Fencemaker thrust belt of central Nevada: *Eos (Transactions, American Geophysical Union)*, v. 80, no. 46, p. F977.
- Wyld, S.J., Rogers, J.W., and Wright, J.E., 2001, Structural evolution within the Luning-Fencemaker fold-thrust belt, Nevada: Progression from back-arc basin collapse to intraarc shortening: *Journal of Structural Geology*, v. 23, p. 1971–1995.
- Wyld, S.J., Rogers, J.W., and Copeland, P., 2002, Metamorphic evolution of the Luning-Fencemaker fold-thrust belt, Nevada:  $^{40}\text{Ar}/^{39}\text{Ar}$  geochronology, illite crystallinity, and metamorphic petrology: *Journal of Geology* (in press).

MANUSCRIPT RECEIVED BY THE SOCIETY 2 APRIL 2001

REVISED MANUSCRIPT RECEIVED 3 DECEMBER 2001

MANUSCRIPT ACCEPTED 4 MARCH 2002

Printed in the USA